INFORMATION TO USERS

This manuscript has been reproduced from the microfilm master. UMI films the text directly from the original or copy submitted. Thus, some thesis and dissertation copies are in typewriter face, while others may be from any type of computer printer.

The quality of this reproduction is dependent upon the quality of the copy submitted. Broken or indistinct print, colored or poor quality illustrations and photographs, print bleedthrough, substandard margins, and improper alignment can adversely affect reproduction.

In the unlikely event that the author did not send UMI a complete manuscript and there are missing pages, these will be noted. Also, if unauthorized copyright material had to be removed, a note will indicate the deletion.

Oversize materials (e.g., maps, drawings, charts) are reproduced by sectioning the original, beginning at the upper left-hand corner and continuing from left to right in equal sections with small overlaps.

Photographs included in the original manuscript have been reproduced xerographically in this copy. Higher quality 6" x 9" black and white photographic prints are available for any photographs or illustrations appearing in this copy for an additional charge. Contact UMI directly to order.

ProQuest Information and Learning
300 North Zeeb Road, Ann Arbor, MI 48106-1346 USA
800-521-0600

Magnetotransport along non parabolically confined quasi-one-dimensional channels

Mario J. Venditti

A Thesis

in

The Department

of

Physics

Presented in Partial Fulfillment of the Requirements

for the Degree of Master of Science at

Concordia University

Montreal, Quebec, Canada

August 2000

Abstract

Magnetotransport along non parabolically confined quasi-one-dimensional channels

Mario J. Venditti

The one-electron spectrum, pertinent to a quantum wire in the presence of a magnetic field,is obtained for parabolic and weakly nonparabolic confining potentials. Different orientations of the magnetic field are considered and the corresponding ac and dc responses of the wire are evaluated, for electron scattering by impurities and/or phonons. The height of the power spectrum peak decreases as the magnetic field is tilted from the normal direction to that along the wire.

Acknowledgments

It is with great pleasure that I would like to express my gratitude to all those who assisted me in the completion of this work.

Special thanks go to my supervisor **Dr. P. Vasilopoulos** whose support, encouragement, advice, and especially patience were greatly appreciated by what must have seemed like a very reluctant student at times.

I would also like to thank the Physics Department of Concordia University for offering me a teaching assistantship. Many thanks to all the fellow students and professors whom I have met during my studies.

Great support was given to me by my family, it is to you that I am eternally grateful.

Table of Contents

List of Figures

Chapter 1

Introduction

1.1 Quantum wires

As electronic devices become smaller and smaller one asks the question how small can they be made and to what purpose? Presently, most devices are essentially two dimensional in nature, effectively confining the electron motion with what is referred to as an inversion layer [1, 20]. Ideally, one would like to create devices that further take advantage of the electron's confinement. Towards this end the ultimate devices would be those in which the electron motion is practically confined to one (quantum wires) or zero (quantum dots) dimensions. This confinement of the electron motion introduces quantum effects that then prove to be useful in the design of electronic devices.

A quantum wire is an electronic device in which the electron is free to travel in one direction only. This confinement leads to a delocalized wave function for the electron which is referred to as an extended state [17].Depending on the mean free path (l_e) of the electron the quantum wire will exhibit different transport properties. If l_e is greater than the length or width of the wire we have what is commonly referred to as ballistic transport [1]. In this regime the extended states exist throughout the length of the wire and the electrons experience only the effect of the confinement potential. The quantum wire acts like a waveguide in this regime. If l_e is smaller than the length of the wire then there could be scattering from impurities. This could lead to the electron being trapped by the impurities into what is called a localized state [17], and so the transport properties would be influenced by the position and number of impurities. Finally, there could be scattering of the electron by phonons, where transport takes place mostly through diffusion of the electron through the material. Simply put, the electron is pushed from one localized state into another by the inelastic scattering with phonons [1]. In all cases, the confinement potential will play a strong role in the electron transport through the wire, by, at the very least modifying the form of the electron wave function.

The quantum wire is constructed from a two-dimensional semiconductor (frequently an AlGaAs/GaAs heterostructure) that has been squeezed in one dimen-

sion [1]-[4]. This squeezing is accomplished using several methods. One method would be etching, where material is physically removed from the semiconductor thus creating a channel where the electrons are made to move in. Another method would be to place a metal split gate on the heterostructure and then apply a negative potential or bias on the metal. This potential would then push the electrons from underneath the split gate essentially creating a one dimensional channel, see Fig. 1.1

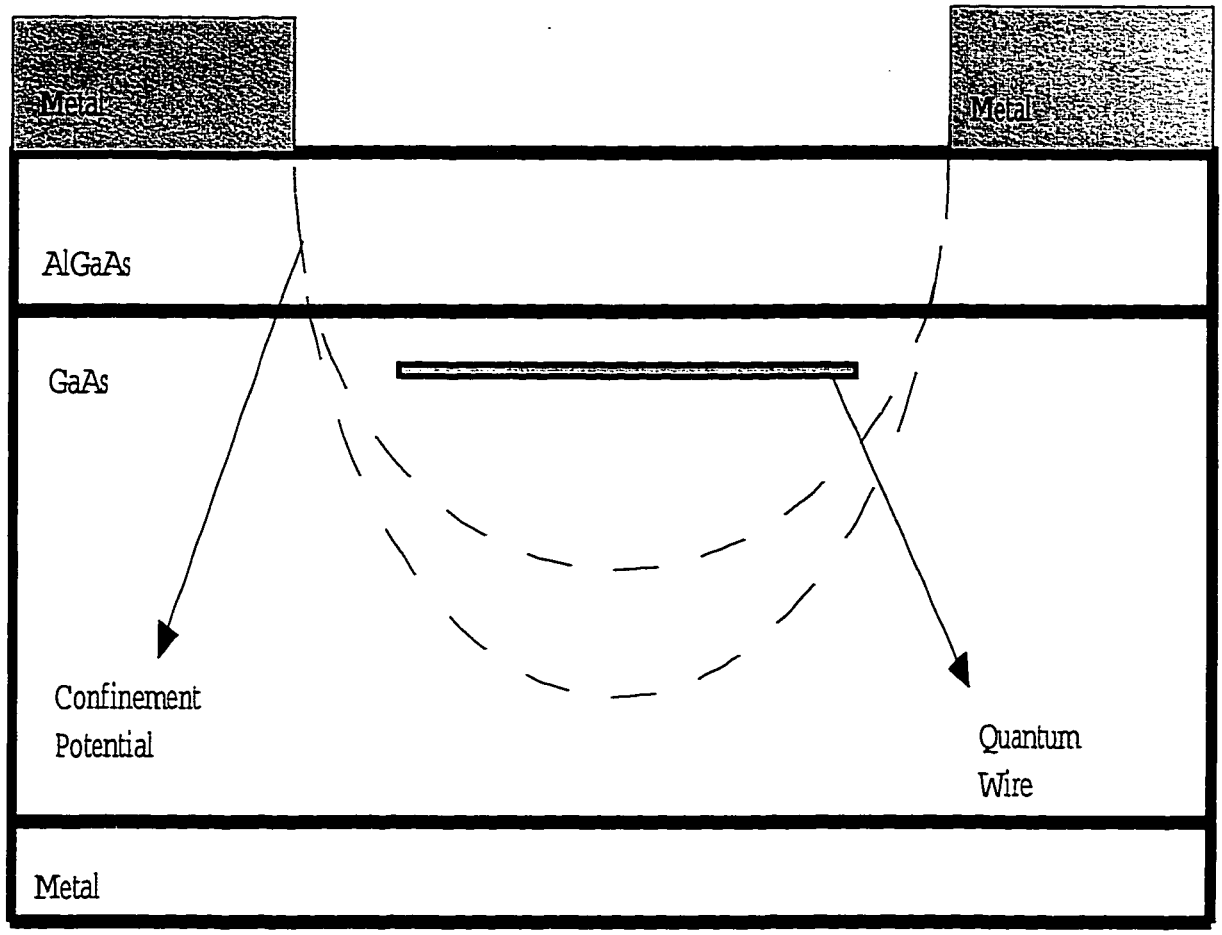

Figure 1.1: Schematic diagram of the front face of a quantum wire. The confinement of the two-dimensional electron gas is done by applying a negative bias across two split gates placed on the top of the AlGaAs/GaAs heterostructure.

1.2 Motivation

Essentially, the form of the confinement potential will affect the transport properties of the quantum wire. If the wire is formed using destructive means, such as etching of the heterostructure, then the confinement potential can be modelled quite accurately using a square well potential [1, 2, 3]. However, when the quantum wire is made using a split gate, then determining the form of the confinement potential is not so straightforward. In most cases the potential is assumed to be harmonic and so the equations of transport theory prove to be analytically tractable.

Difficulties are encountered when the form of the confinement potential is determined using self-consistent calculations [5]- [7]; they show that, in addition to the harmonic term, there must be higher-order terms present in the confinement potential especially as the gate voltage is decreased. If the form of the latter found using the self-consistent calculations is used to determine the transport properties, the equations of linear transport theory are no longer tractable and numerical methods must be used. Furthermore, power spectrum results [26] in the edge states of a two dimensional electron gas show that the confinement of one dimensional systems is essentially harmonic with small anharmonic terms present.

As a result, we try and model the confinement potential using the harmonic

potential with the addition of small higher-order terms. This enables us to treat the problem as a harmonic one with small corrections using perturbation theory. This would render the relevant transport formulas fairly tractable and the end result might be closer to what is found when the full self-consistent theory is used.

1.3 Outline

The work is organized as follows. In chapter 2, we study the problem of the energetics of a free electron gas. Schrödinger's one-electron equation is solved for various orientations of the magnetic field using the method of separation of variables. The correction to the confinement is introduced for the magnetic field perpendicular to the plane of the wire as well as parallel to the wire. In these two cases perturbation theory can be used to determine the correction to the eigenvalues and wave functions. These results are used to determine the density of states for the different orientations of the magnetic field.

Chapter 3 deals with the response of the wire to an applied d.c. current. The conductivity tensor is calculated for various scattering potentials, both elastic and inelastic. Numerical results are obtained for the conductivity tensors when results about the form of the confinement potential can be inferred.

In chapter 4 we study the power spectrum of the wire or the response of the

wire to an applied a.c. current. The conductivity tensors are found in a general form for each orientation of the magnetic field. This can be done because the non-diagonal components needed for the calculation of the power spectrum deal solely with the energy difference between subbands. The power spectrum of the anharmonic potential is compared to that of the harmonic one.

Chapter 5 summarizes the conclusions of the thesis and discuses possible further areas of study.

Chapter 2

Schrödinger Equation

In order to determine the response of the wire to external fields (magnetic and electric), we can work within the framework of linear response theory, and in particular the Kubo-Greenwood Formulas. These formulas make use of the single electron approximation. Accordingly, the many-electron system is treated in an average or Hartree sense, i.e. as a noninteracting Fermi gas. As a result, the evaluation of these formulas requires the energy and wave function of a single-electron.

In the following chapter we solve the Schrödinger equation for various orientations of the magnetic field. We assume that the confinement potential of the quantum wire is a harmonic one, making it possible to diagonalize the Schrödinger equation. This enables us to use the method of separation of variables to determine

its eigenvalues and eigenfunctions. Small corrections (cubic and higher order) to the confinement potential are then treated using perturbation theory.

The results are used to find the density of states (DOS), which would then tell us something about the relative effect of the different confining potentials.

2.1 Magnetic field perpendicular to the wire

We consider a quantum wire in the x-y plane, with the electron motion along the x-axis and a magnetic field perpendicular to the (x,y) plane of the wire. The Schrödinger equation [9, 8] is given by

$$\frac{1}{2m}\left[\frac{\hbar\nabla}{i} - e\vec{A}\right]^2 \Psi + V(y)\Psi = \epsilon\Psi \tag{2.1}$$

The function $V(y)$, is used to model the confining potential of the wire along the y axis. This confining potential breaks the symmetry that would normally exist for a two dimensional device, i.e. we are limited to those vector potentials $\vec{A}$ that will not confine the motion of the electron in the x direction. As a result, we choose a Landau gauge of the form $\vec{A} = (-By, 0, 0)$ which results in a magnetic field that is in the z direction and does not confine the motion of the electron along the x axis.

Assuming solutions of the form $\Psi(x, y) = AU(y)\exp(ik_x x)$ the Schrödinger

equation can be rewritten in the form

$$\frac{-\hbar^2}{2m}\frac{d^2U(y)}{dy^2} + \frac{m}{2}\omega_c^2(y - \frac{\hbar k_x}{m\omega_c})^2 U(y) + V(y)U(y)$$

$$= \left[\epsilon - \frac{\hbar^2 k_x^2}{2\tilde{m}}\right] U(y) \tag{2.2}$$

where $\omega_c = eB/m$ is the cyclotron frequency. Equation (2.2) can be solved analytically for a harmonic confining potential $V(y) = m\Omega^2 y^2/2$. The energy eigenvalue is then given by

$$\epsilon = (n + 1/2)\hbar\varpi + \frac{\hbar^2 k_x^2}{2\tilde{m}}, \tag{2.3}$$

with the effective mass $\tilde{m} = (m\varpi^2)/(\varpi^2 - \omega_c^2)$ and $\varpi^2 = \omega_c^2 + \Omega^2$. The wave functions (eigenfunctions) are of the form

$$\Psi(x, y) = |n, k_x\rangle =$$
$$\sqrt{\frac{\alpha}{\sqrt{\pi}2^n n! L_x}} H_n[\alpha(y - y_0)] \exp(-\frac{\alpha^2(y - y_o)^2}{2} + \imath k_x x) \tag{2.4}$$

where $\alpha = \sqrt{m\varpi/\hbar}$. In the following we model the confinement $V(y)$ using a parabolic potential with the addition of smaller higher order terms. In the first case $V(y) = m\Omega^2 y^2/2 + \lambda y^3$ and in the second one, $V(y) = m\Omega^2 y^2/2 + \lambda y^3 + \gamma y^4$. A linear term βy is not added because it would result in a constant shift of the energy levels and would reappear only in the arguement as a shift in the center of

cyclotron orbit. This shift in energy and orbit center could then be absorbed into the y_o term with a simple change in coordinate axes.

2.1.1 Cubic corrections to the confining potential

Inserting $V(y) = m/2\Omega^2 y^2 + \lambda y^3$ into the Schrödinger equation (2.2) and making the substitution $y' = y - y_o$ gives the equation

$$\frac{-\hbar^2}{2m}\frac{d^2U(y'-y_o)}{dy'^2} + \frac{m}{2}\varpi y'^2 U(y'-y_o)$$

$$+\lambda\left[y'^3 + 3y_o^2 y' + 3y_o y'^2\right]U(y'-y_o) = \epsilon' U(y'-y_o). \tag{2.5}$$

The energy eigenvalue $\epsilon' = \epsilon - \hbar^2 k_x^2/2\tilde{m} - \lambda y_o^3$, and $y_o = b\tilde{l}^2 k_x$, with $b = \omega_c/\varpi$, and $\tilde{l}^2 = \hbar/m\varpi$.

The Hamiltonian can be considered to be the sum of H_o, which is the one-dimensional harmonic oscillator with solution Eq.(2.4), and a perturbation $H_1 = \lambda[y'^3 + 3y_o^2 y' + 3y_o y'^2]$. The energy eigenvalue of the unperturbed Hamiltonian is

$$\epsilon^{(0)} = (n + \frac{1}{2})\hbar\varpi + \frac{\hbar^2 k_x^2}{2\tilde{m}} + \lambda y_o^3. \tag{2.6}$$

The perturbed Hamiltonian, H_1, cannot be diagonalized but can be approximated using perturbation theory[9, 8, 10]. Also, H_1 is the sum of an odd (y'^3 +

$3y_o^2y'$) and an even ($3y_oy'^2$) function of y' and so by the recursion relations and orthogonality properties of the Hermite polynomials the odd function would give zero first-order corrections to the energy. The first-order energy corrections of the even function are

$$\epsilon^{(1)} = \lambda\langle n, k_x|3y_oy'^2|n, k_x\rangle. \tag{2.7}$$

The above expression can be simplified quite readily to give

$$\epsilon^{(1)} = \frac{3\lambda y_o}{\alpha^2}(n + \frac{1}{2}). \tag{2.8}$$

The second-order correction to the energy eigenvalues is given by

$$\epsilon^{(2)} = \sum_{n\neq m} \frac{\langle n, k_x|H_1|m, k_x\rangle\langle m, k_x|H_1|n, k_x\rangle}{E_n - E_m}, \tag{2.9}$$

where H_1 is the perturbed Hamiltonian. This expression can be evaluated by expanding $H_1|n, k_x\rangle$ using the recursion relation of the Hermite polynomials. Then the matrix $\langle m, k_x|H_1|n, k_x\rangle$ can be simplified using the orthogonality properties and Eq. (2.9) to give

$$\epsilon^{(2)} = -\frac{\lambda^2}{8\alpha^6\hbar\varpi}[3n^2 + 3n + 2 + 9\,(n+1)\left[n + \left(1 + 2\alpha^2y_o^2\right)\right]^2 +$$

$$-9n\left(n + 2\alpha^2y_o^2\right)^2] + \frac{-9\lambda^2y_o^2}{2\alpha^4\hbar\varpi}. \tag{2.10}$$

Hence, the eigenvalue of the complete Hamiltonian $H_o + H_1$ is

$$\epsilon = (n + \frac{1}{2})\hbar\varpi + \frac{\hbar^2k_x^2}{2\tilde{m}} + \epsilon^{(1)} + \epsilon^{(2)} + \lambda y_o^3. \tag{2.11}$$

A plot of the eigenvalue as a function of the wave vector k_x is shown in Fig. 2.1.

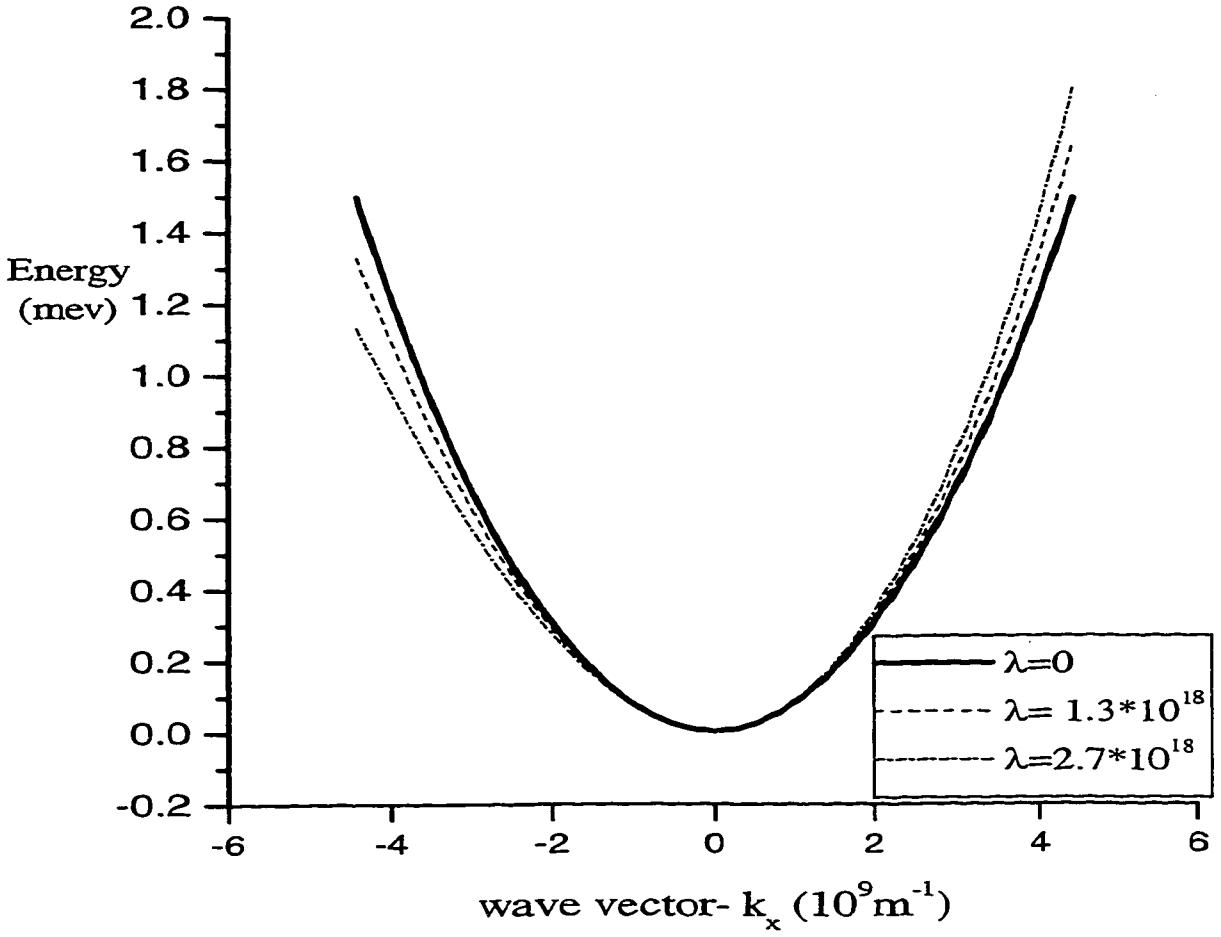

Figure 2.1: Energy eigenvalues as a function of the wave vector k_x with $n = 0$. λ has units of eV/m^3

The corrected wave function has both first and second-order corrections. The first-order corrections are given by

$$|n,k_x\rangle^1 = \sum_{m\neq n} \frac{\langle nk_x|H_1|mk_x\rangle}{E_n - E_m}|m,k_x\rangle^{(0)}; \tag{2.12}$$

the second order corrections can be ignored because they will not contribute much to any of the expectation values $\langle n,k_x|^{(2)}X|n,k_x\rangle^{(2)} \to \lambda^4$ where X is any operator and λ is the strength of the perturbation. Also, the cross terms between the first and second-order corrections can be ignored because they will give terms of order λ^3.

With these details Eq. (2.12) can be evaluated using the matrix $\langle n,k_x|H_1|m,k_x\rangle$ that was found for the energy corrections to give

$$|n,k_x\rangle^1 = \frac{\lambda\sqrt{n\,(n-1)\,(n-2)}}{3\alpha^3\hbar\varpi}|n-3,k_x\rangle + \frac{3\lambda y_o}{4\alpha^2\hbar\varpi}\sqrt{\frac{n\,(n-1)}{2}}|n-2,k_x\rangle$$

$$+\frac{3\lambda y_o}{\alpha\hbar\varpi}\sqrt{\frac{n}{2}}\left[\frac{n}{2\alpha^2}+y_o^2\right]|n,k_x\rangle + -\frac{3\lambda y_o}{\alpha\hbar\varpi}\sqrt{\frac{(n+1)}{2}}\left[\frac{(n+1)}{2\alpha^2}+y_o^2\right]|n+1,k_x\rangle$$

$$-\frac{3\lambda y_o}{4\alpha^2\hbar\varpi}\sqrt{\frac{(n+2)\,(n+1)}{2}}|n+2,k_x\rangle$$

$$+\frac{-\lambda\sqrt{(n+3)\,(n+2)\,(n+1)}}{3\alpha^3\hbar\varpi}|n+3,k_x\rangle \tag{2.13}$$

2.1.2 Fourth-degree polynomial correction to the confining potential

Inserting the potential $V(y) = m\Omega^2 y^2/2 + \lambda y^3 + \gamma y^4$ into Eq.(2.2) gives

$$\frac{-\hbar^2}{2m}\frac{d^2U(y'-y_o)}{dy'^2} + \frac{m}{2}\omega' y'^2 U(y'-y_o)$$

$$+\left[\gamma y'^4 + \Gamma y'^3 + \Lambda y'^2 + \Upsilon y'\right] U(y'-y_o) = \epsilon' U(y'-y_o), \tag{2.14}$$

where $\Gamma = \lambda + 4\gamma y_o$, $\Lambda = 3\lambda y_o + 6\gamma y_o^2$, and $\Upsilon = 3\lambda y_o^2 + 6\gamma y_o^3$. The eigenvalues are

$$\epsilon' = \epsilon - \frac{\hbar^2 k_x^2}{2\tilde{m}} - \lambda y_o^3 - \gamma y_o^4. \tag{2.15}$$

As in the correction to the cubic term in the previous section, we have H_o, the Hamiltonian for the one-dimensional harmonic oscillator, and a perturbation H_1. The first-order corrections to the energy are given by

$$\epsilon^1 = \langle nk_x|\gamma y'^4 + \Gamma y'^3 + \Lambda y'^2 + \Upsilon y'|nk_x\rangle. \tag{2.16}$$

Expanding H_1 using the recursion relations of the Hermite polynomials, only the even functions will contribute to the energy. The result is

$$\epsilon^{(1)} = \frac{\gamma}{2\alpha^4}\left[n^2 - n + 1\right] + \frac{\gamma}{\alpha^4}(n+1)^2 + \frac{\Lambda}{\alpha^2}(n+\frac{1}{2}). \tag{2.17}$$

The second-order energy correction is found using Eq. (2.9); it is given by

$$\epsilon^{(2)} = \frac{-\Gamma^2(n+3)(n+2)(n+1)}{24\alpha^6\hbar\varpi} + \frac{\Gamma^2(n-2)(n-1)n}{24\alpha^6\hbar\varpi}$$

$$-\frac{n+1}{2\hbar\varpi}\left(\frac{3(n+1)\Gamma}{2\alpha^3}+\frac{\Upsilon}{\alpha}\right)^2 + \frac{n}{2\hbar\varpi}\left(\frac{3n\Gamma}{2\alpha^3}+\frac{\Upsilon}{\alpha}\right)^2. \tag{2.18}$$

Thus the corrected energy eigenvalue is

$$\epsilon = (n+\frac{1}{2})\hbar\varpi + \frac{\hbar^2 k_x^2}{2\tilde{m}} + \lambda y_o^3 + \gamma y_o^4 + \epsilon^{(1)} + \epsilon^{(2)}. \tag{2.19}$$

A plot of the eigenvalue as a function of the wave vector k_x is shown in Fig. 2.2.

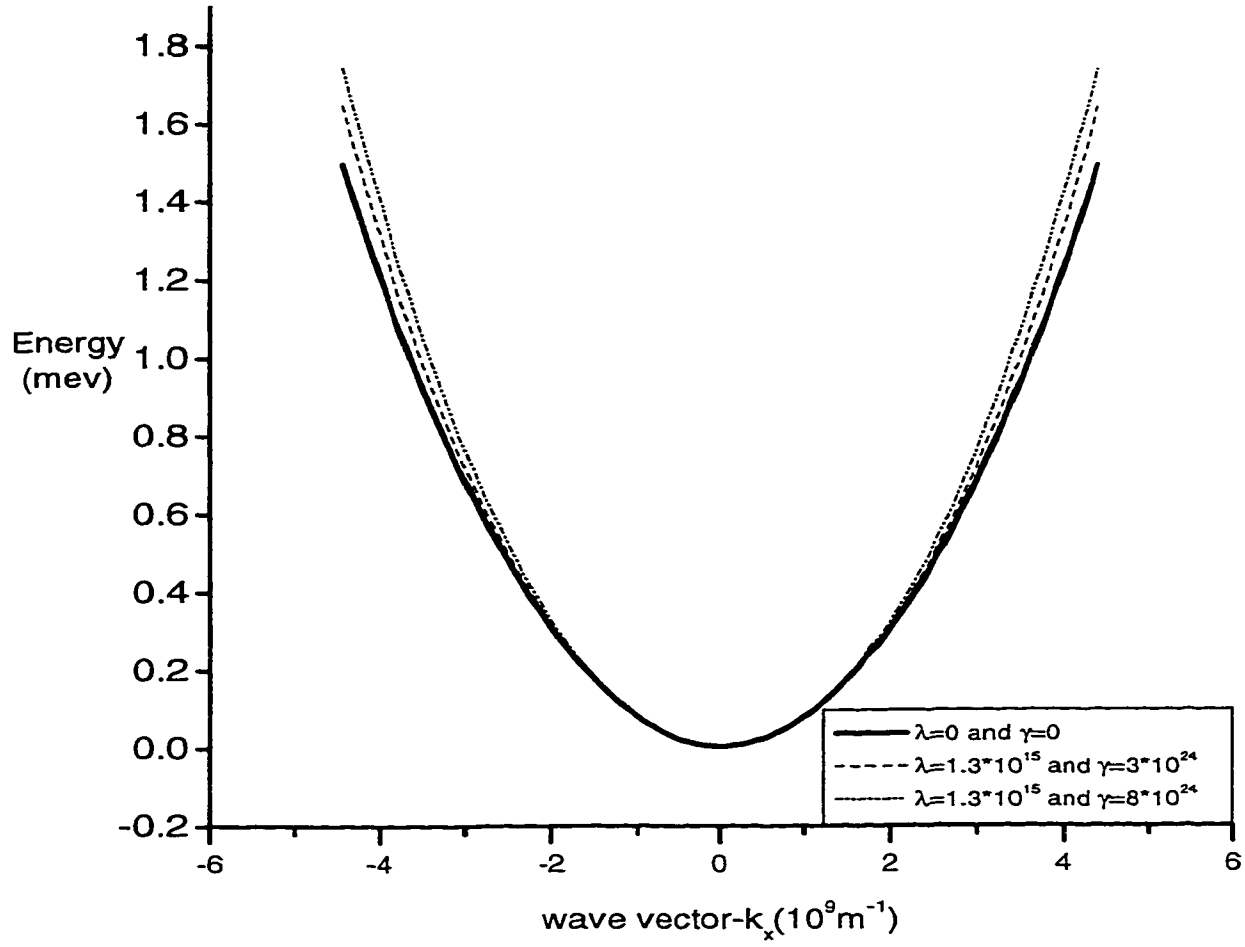

Figure 2.2: Energy eigenvalues as a function of the wave vector k_x with $n = 0$. λ has units of eV/m^3 and γ has units of eV/m^4.

2.1.3 Density of States

The density of states (DOS) for the three separate energy spectrums has an exact solution for the harmonic oscillator but must be solved numerically for the two perturbed problems. The general form of the DOS [11] is

$$D(\epsilon) = 2\sum_n \frac{L_x}{2\pi}\int dk_x \delta(\epsilon - \epsilon_n(k_x)) \tag{2.20}$$

where L_x is the length of the quantum wire.Inserting the energy eigenvalue of the harmonic oscillator, Eq. (2.3) into the above equation results in

$$\frac{D(\epsilon)}{L_x} = \frac{1}{\pi}\sum_n \int dk_x \delta(\epsilon - (n+1/2)\hbar\varpi - \frac{\hbar^2 k_x^2}{2\tilde{m}}). \tag{2.21}$$

Making the substitution $v = \hbar^2 k_x^2/2\tilde{m}$, the integral can readily be solved to give

$$D(\epsilon) = \sqrt{\frac{\tilde{m}}{2\pi^2\hbar^2}}\sum_n \frac{1}{\sqrt{E}} \tag{2.22}$$

with $E = \epsilon - (n+1/2)\hbar\varpi$. If, however, Lorentzian broadening of the DOS is introduced, i.e. if the change $\delta(\epsilon - \epsilon_{n,k_k}) \rightarrow \Gamma/\pi[(\epsilon - \epsilon_{n,k_x})^2 + \Gamma^2]$ is made , then the DOS becomes

$$D(\epsilon) = \frac{1}{\pi}\int dk \frac{\Gamma/\pi}{(\epsilon - \epsilon_n(k_x))^2 + \Gamma^2}. \tag{2.23}$$

This expression can be evaluated analytically [12] for the harmonic oscillator; the result is

$$D(\epsilon) = \frac{1}{\pi^2\hbar}\sum_n \sqrt{\frac{\tilde{m}}{2}}\frac{\cos(\frac{\alpha}{2})}{(E^2+\Gamma^2)^{\frac{1}{4}}} \times$$

$$\left[\tan(\frac{\alpha}{2})\ln\left(\frac{k^2+2qk\cos(\frac{\alpha}{2})+q^2}{k^2-2qk\cos(\frac{\alpha}{2})+q^2}\right) + 2\arctan\left(\frac{k^2-q^2}{2qk\sin(\frac{\alpha}{2})}\right)\right] \quad (2.24)$$

where, $E = \epsilon - (n+1/2)\hbar\varpi$, $q = (\tilde{m}^2(E^2+\Gamma^2)/\hbar^4)^{\frac{1}{4}}$, $\cos\alpha = E/\sqrt{E^2+\Gamma^2}$, and $\sin\alpha = \Gamma/\sqrt{E^2+\Gamma^2}$. If it is the DOS for the perturbed energy spectrum that we are looking for, then we replace the energy eigenvalue above with the energy eigenvalues given by Eq.(2.11) and (2.19) and evaluate numerically.

As seen in Fig.2.3, the DOS for the different confining potentials is almost identical, so much so that we may estimate the DOS for all corrected potentials with the DOS for the harmonic problem. This will greatly simplify further calculations, e.g. that of the Fermi energy without there being any appreciable difference in the final result.

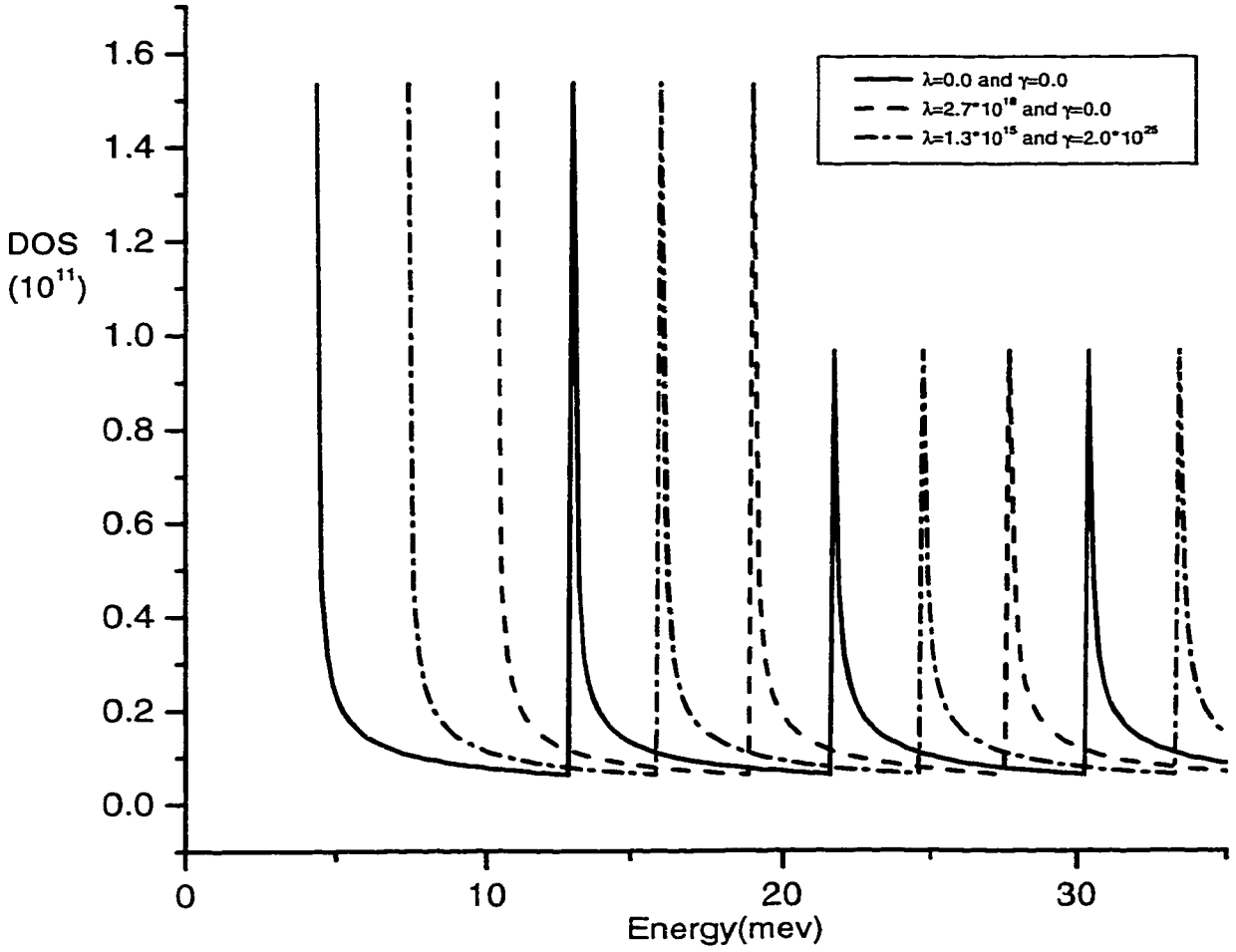

Figure 2.3: DOS for different forms of the confining potential. The dashed lines are the DOS for a cubic and fourth-order correction to the harmonic potential. The strength of the perturbations is approximately 20% that of the harmonic potential. The corrected potentials have been shifted along the x axis for clarity. λ has units of eV/m^3 and γ has units of eV/m^4.

2.2 Magnetic field parallel to the wire axis

We consider the gauge $\vec{A} = (0, 0, By)$, which gives a magnetic field in the x direction, parallel to the electron motion. Inserting this $\vec{A}$ into the Schrödinger Eq. (2.1) gives

$$-\frac{\hbar^2}{2m}\frac{\partial^2\Psi}{\partial x^2} - \frac{\hbar^2}{2m}\frac{\partial^2\Psi}{\partial y^2} + e^2B^2y^2\Psi + V(y)\Psi = \epsilon\Psi \tag{2.25}$$

As in the case where the magnetic field is perpendicular to the wire, exact solutions to the above equation can be found for $V(y) = m\Omega^2y^2/2$. When plane wave solutions are assumed in the x direction then the resulting equation for y is nothing more than the quantum harmonic oscillator with $\varpi^2 = \Omega^2 + \omega_c^2$. Solutions for the wave equation are

$$\Psi(x, y) = |nk\rangle = \sqrt{\frac{1}{L_x\sqrt{\pi}l2^n n!}}H_n(y)\exp(-\frac{y^2}{2l^2} + \imath k_x x), \tag{2.26}$$

and the eigenvalue

$$\epsilon = (n + \frac{1}{2})\hbar\varpi + \frac{\hbar^2k_x^2}{2m} \tag{2.27}$$

where $l = \hbar/m\varpi$.

2.2.1 Cubic corrections to the confining potential

When a non-parabolic term $V(y)$ is introduced into the Hamiltonian then the eigenvalues and eigenfunctions can be obtained using perturbation theory. We

consider the confining potential $V(y) = m\Omega^2 y^2/2 + \lambda y^3$ which allows us to split the Hamiltonian into a harmonic oscillator part H_o and a perturbation $H_1 = \lambda y^3$. Due to the orthogonality of the Hermite polynomials [9, 10], H_1 must be treated using second-order perturbation theory. The corrections to the energy eigenvalues are found by inserting H_1 into Eq. (2.9),

$$\epsilon^{(2)} = \sum_{m \neq n} \frac{\langle nk|\lambda y^3|mk'\rangle\langle mk'|\lambda y^3|nk\rangle}{\epsilon^0_{nk} - \epsilon^0_{mk'}}. \tag{2.28}$$

The evaluation of this formula gives

$$\epsilon^{(2)} = -\frac{\lambda^2 l^6}{8\hbar\omega}[30n^2 + 30n + 11] \tag{2.29}$$

for the correction to the eigenvalue. The energy eigenvalue for the complete Hamiltonian, $H_o + H_1$, is given by

$$\epsilon = (n + \frac{1}{2}) + \frac{\hbar^2 k_x^2}{2m} - \frac{\lambda^2 l^6}{8\hbar\omega}[30n^2 + 30n + 11]. \tag{2.30}$$

A plot of the eigenvalue as a function of the wave vector k_x is shown in Fig. 2.4 for $n = 0$.

The corrections to the wave function follow the same procedure as in the $B \perp$ case where, the first-order corrections are given by Eq. (2.12); the second-order corrections can be neglected because their contribution is of order λ^2. Therefore, inserting H_1 into Eq. (2.12) and simplifying gives

$$|n,k_x\rangle^{(1)} = \frac{\lambda l^3}{\hbar\varpi}[\sqrt{\frac{n(n-1)(n-2)}{72}}|n-3,k_x\rangle + \sqrt{\frac{9n^3}{8}}|n-1,k_x\rangle$$

$$-\sqrt{\frac{9(n+1)^3}{8}}|n+1,k_x\rangle - \sqrt{\frac{(n+3)(n+2)(n+1)}{72}}|n+3,k_x\rangle] \quad (2.31)$$

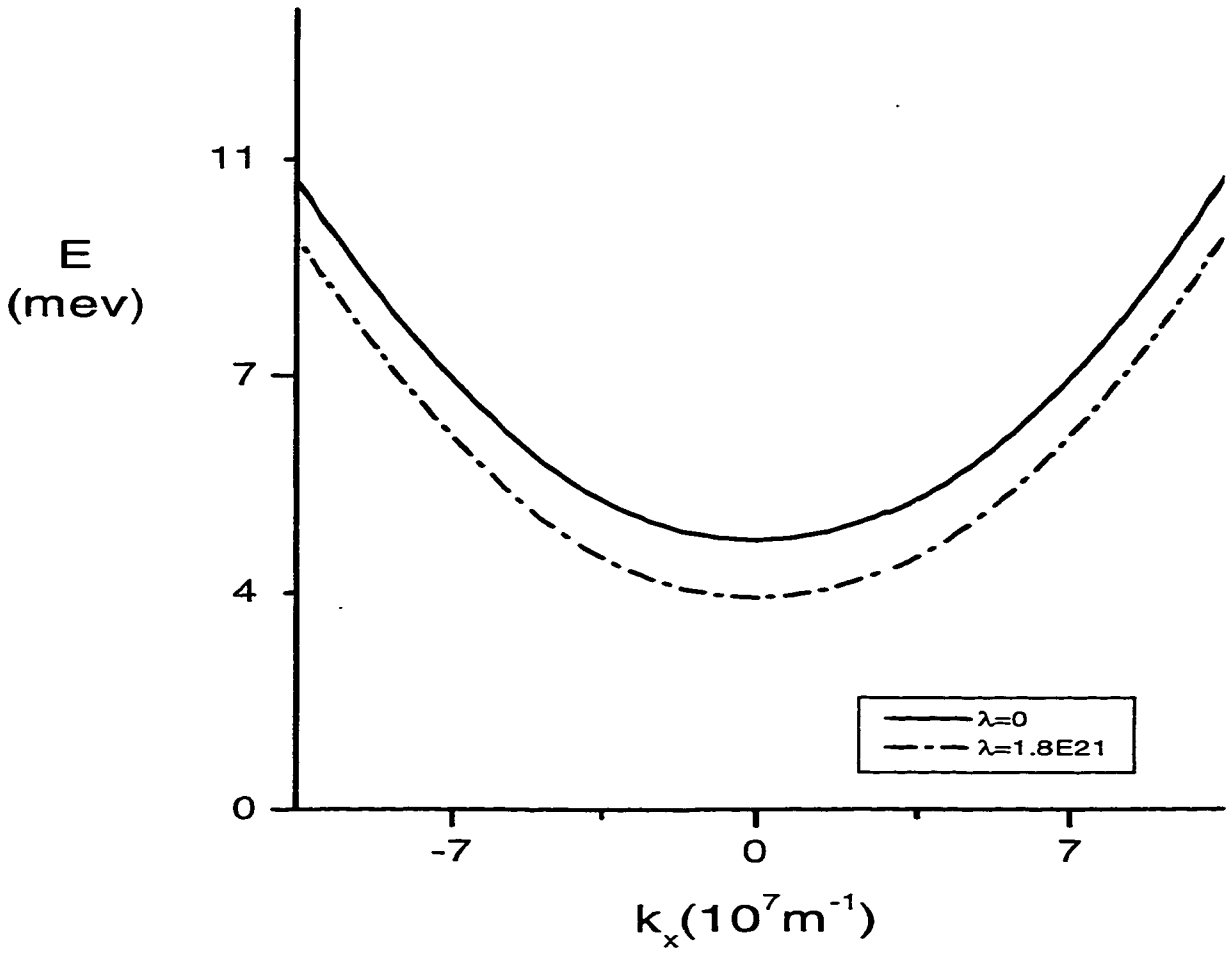

Figure 2.4: Eigenvalues as a function of the wave vector k_x with $n = 0$. λ has units of eV/m^3.

2.2.2 Fourth-degree polynomial correction to the confining potential

The confining potential of the quantum wire is modeled by adding $V(y) = \frac{m\Omega^2}{2}y^2 + \lambda y^3 + \gamma y^4$ to the Hamiltonian of Eq. (2.25). As in the case with the cubic term, the Hamiltonian can be divided into a harmonic oscillator part, H_o,and a perturbation H_1. First and second-order perturbation theory is used in order to obtain the corrections to the eigenvalues. The first-order corrections are given by

$$\epsilon^{(1)} = \langle n, k_x | \lambda y^3 + \gamma y^4 | n, k_x \rangle. \tag{2.32}$$

Expanding $V(y)$ using the recursion relations [9, 10] and simplifying with the orthogonality of the Hermite polynomials gives

$$\epsilon^{(1)} = \frac{3\gamma l^4}{4}\left[2n^2 + 2n + 1\right]. \tag{2.33}$$

The second-order corrections to the eigenvalues are found by inserting $V(y)$ into Eq. (2.30). The result is

$$\epsilon^{(2)} = \sum_{m \neq n} \frac{\langle nk | \gamma y^4 + \lambda y^3 | mk' \rangle \langle mk' | \gamma y^4 + \lambda y^3 | nk \rangle}{\epsilon^0_{nk} - \epsilon^0_{mk'}}. \tag{2.34}$$

A straightforward evaluation gives

$$\epsilon^{(2)} = -\frac{\lambda^2 l^6}{8\hbar\varpi}\left[30n^2 + 30n + 11\right] + \frac{\gamma^2 l^8}{8\hbar\varpi}\left[2n^3 + 3n^2 + 7n + 3\right] \tag{2.35}$$

The energy eigenvalue for the complete Hamiltonian, $H_o + H_1$, is

$$\epsilon = (n + \frac{1}{2}) + \frac{\hbar^2 k_x^2}{2m} + \epsilon^{(1)} + \epsilon^{(2)}. \tag{2.36}$$

A plot of the eigenvalue as a function of the wave vector k_x is shown in Fig. 2.5 for $n = 0$.

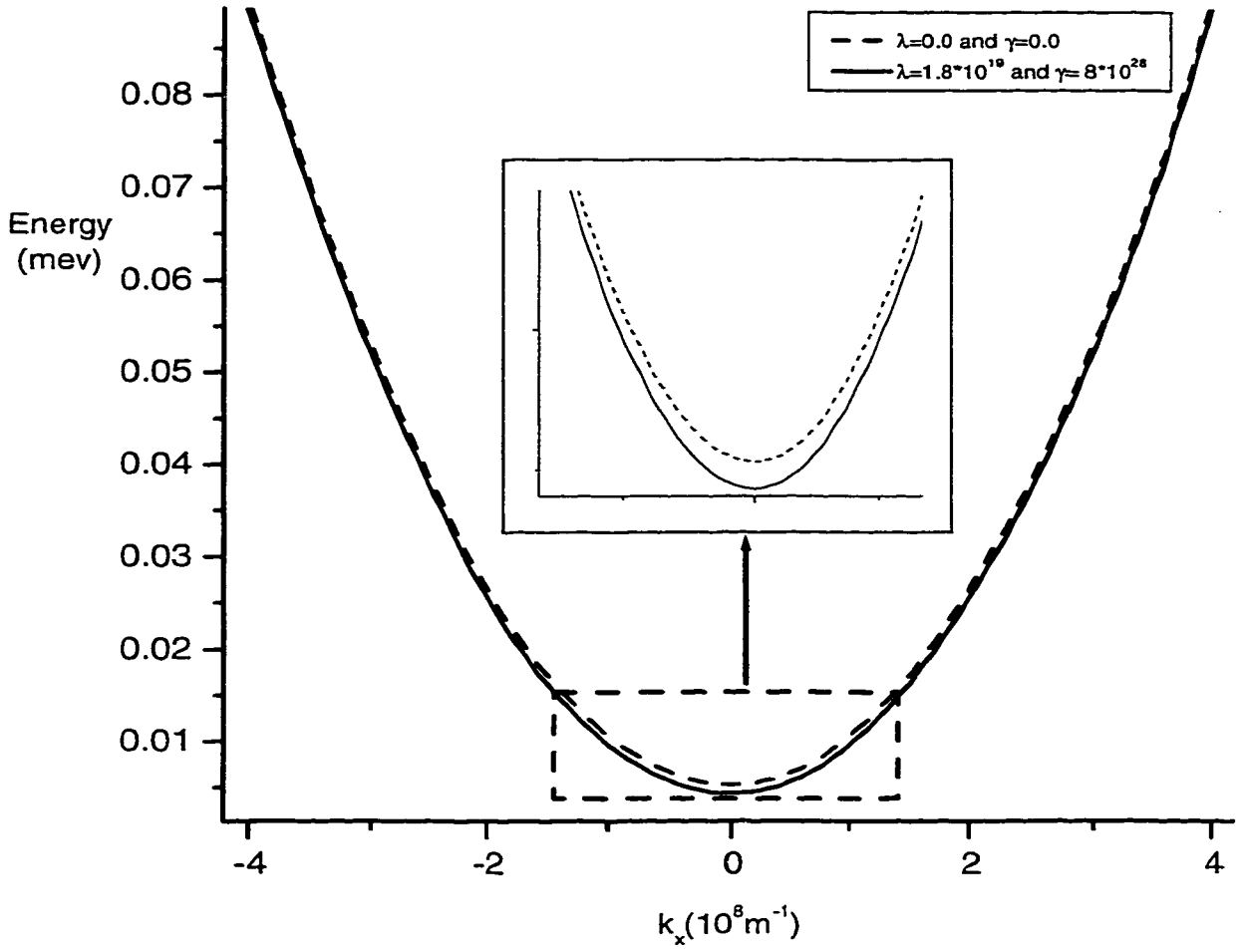

Figure 2.5: Eigenvalues as a function of the wave vector k_x with $n = 0$. Again λ has units of eV/m^3 and γ has units of eV/m^4.

2.2.3 Density of States

The procedure for finding the DOS is identical to that for the magnetic field perpendicular to the wire. Using Eq. (2.20) and the eigenvalue Eq. (2.27), the DOS is

$$D(\epsilon) = \sqrt{\frac{m}{2\pi^2\hbar^2}} \sum_n \frac{1}{\sqrt{E}}, \tag{2.37}$$

with $E = \epsilon - (n + \frac{1}{2})\hbar\varpi$. When a Lorentzian broadening is introduced then the DOS is found using Eq. (2.23). The DOS then is

$$D(\epsilon) = \frac{1}{\pi^2\hbar}\sqrt{\frac{m}{2}} \sum_n \frac{\cos(\frac{\alpha}{2})}{(E^2+\Gamma^2)^{\frac{1}{4}}}$$

$$\times \left[\tan(\frac{\alpha}{2}) \ln\left(\frac{k^2 + 2qk\cos(\frac{\alpha}{2}) + q^2}{k^2 - 2qk\cos(\frac{\alpha}{2}) + q^2}\right) + 2\arctan\left(\frac{k^2 - q^2}{2qk\sin(\frac{\alpha}{2})}\right)\right], \tag{2.38}$$

with $q = (m^2(E^2+\Gamma^2)/\hbar^4)^{\frac{1}{4}}$, $\cos\alpha = E/\sqrt{E^2+\Gamma^2}$, and $\sin\alpha = \Gamma/\sqrt{E^2+\Gamma^2}$.

The DOS for the confining potential with higher-order terms must be solved numerically. The result of Fig. 2.6 is identical to that found for the magnetic field perpendicular to the quantum wire. Again the small change in the confining potential does not have an appreciable effect on the DOS. As a result, we can use the DOS for the harmonic potential as an estimate in all further calculations.

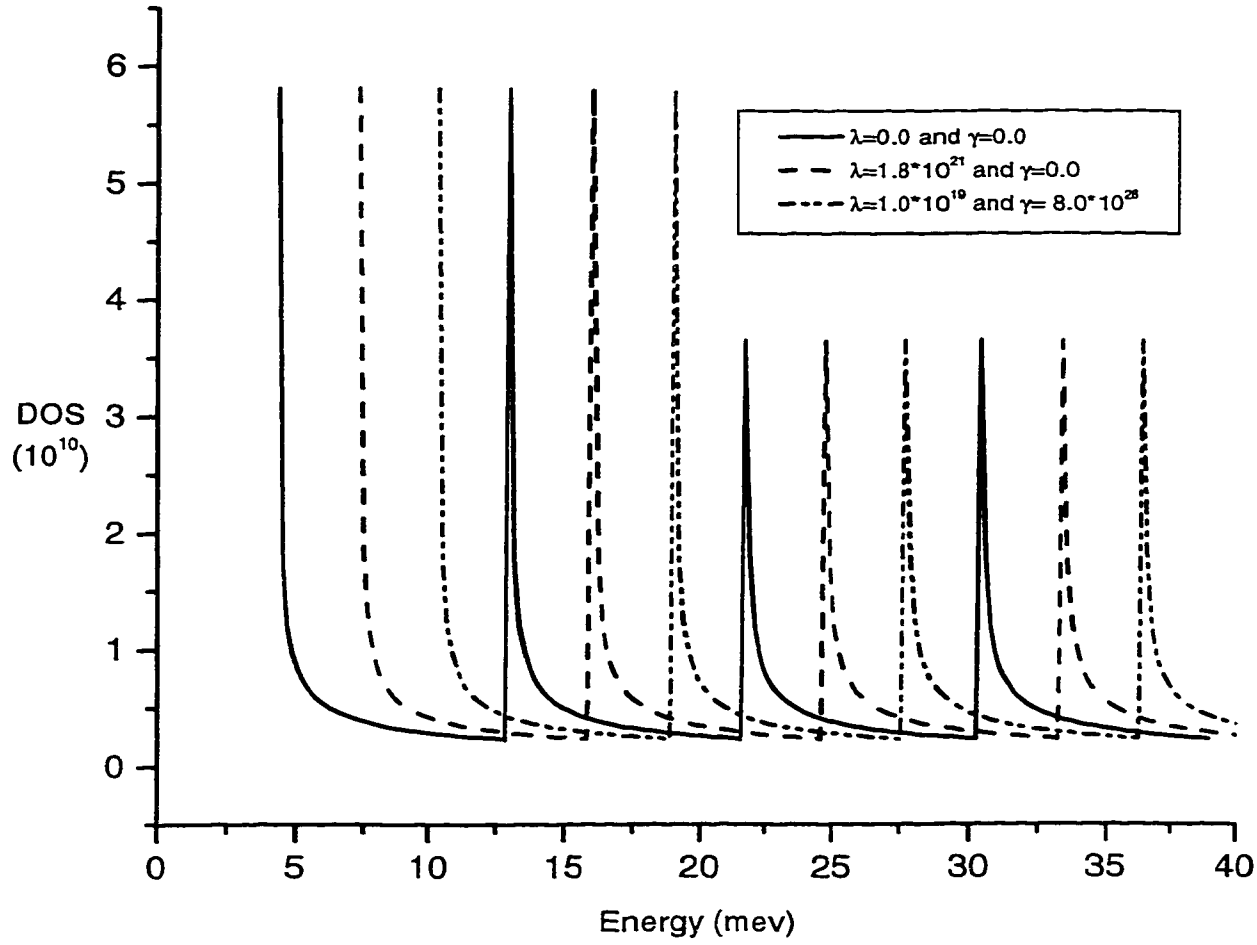

Figure 2.6: The DOS for three different confining potentials(shifted along the x axis). A perturbation of up to 20% of the harmonic confinement has little effect upon the DOS. λ has units of eV/m^3 and γ has units of eV/m^4.

2.3 Magnetic field that is in the plane but perpendicular to a wire of finite thickness

We consider a model of a wire that has finite thickness in the z axis . This extra dimension affords us greater freedom in picking a gauge that will diagonalize the Schrödinger equation and leaves the electron free to move in one of the directions (along the x axis). We consider the confining potential $V(y,z) = m\left[\Omega_y^2 y^2 + \Omega_z^2 z^2\right]/2$ such that $\Omega_z \gg \Omega_y$, essentially making the wire much thinner along the z axis. The gauge $\vec{A} = (-Bz, 0, 0)$ gives a magnetic field in the y direction and inserting it into the Schrödinger equation gives

$$-\frac{\hbar^2}{2m}\frac{\partial^2\Psi}{\partial x^2} + -\frac{\hbar^2}{2m}\frac{\partial^2\Psi}{\partial y^2} - \frac{\hbar^2}{2m}\frac{\partial^2\Psi}{\partial z^2} + e^2B^2y^2\Psi +$$

$$+\frac{m}{2}[\Omega_y^2 y^2 + \Omega_z^2 z^2]\Psi + \frac{m}{2}\omega_c^2 z^2 - i\hbar\omega z\frac{\partial\Psi}{\partial x} = \epsilon\Psi \qquad (2.39)$$

This Schrödinger equation is separable if solutions are of the form $\Psi(x,y,z) = CZ(z)Y(y)\exp(ik_x x)$. Inserting $\Psi(x,y,z)$ into Eq. (2.39) we obtain two equations both one-dimensional harmonic oscillators. The wave function for the Schrödinger equation is

$$\Psi(x,y,z) = \frac{H_s[\frac{z+bl_s^2k_x}{l_s}]H_n[-\frac{y}{l_n}]}{\sqrt{\pi 2^{n+s}n!s!l_n l_s}}\exp\left[ik_x x - \frac{(z+bl^2k_x)^2}{2l_s^2} - \frac{y^2}{2l_n^2}\right], \qquad (2.40)$$

and the eigenvalue

$$\epsilon = \left[s + \frac{1}{2}\right] \hbar\varpi + \left[n + \frac{1}{2}\right] \hbar\Omega_y + \frac{\hbar^2 k_x^2}{2\tilde{m}}, \tag{2.41}$$

where $\tilde{m} = m[\varpi/\Omega_c]^2$, $l_s = \sqrt{\hbar/m\varpi}$, $b = \omega_c/\varpi$, and $l_n = \sqrt{\hbar/m\Omega_y}$.

2.3.1 Density of States

Insertion of Eq. (2.41) into Eq. (2.20) and following the same procedure before gives

$$D(\epsilon) = \sqrt{\frac{\tilde{m}}{2\pi^2\hbar^2}} \sum_n \sum_s \frac{1}{\sqrt{E}}, \tag{2.42}$$

where $E = \epsilon - (s + 1/2)\,\hbar\varpi - (n + 1/2)\,\hbar\Omega_y$. The Lorenztian broadened DOS is also treated in the same manner as before. Inserting the eigenvalue (2.41) into Eq. (2.23) we obtain

$$D(\epsilon) = \frac{1}{\pi^2\hbar}\sqrt{\frac{\tilde{m}}{2}} \sum_n \sum_s \frac{\cos(\frac{\alpha}{2})}{(E^2 + \Gamma^2)^{\frac{1}{4}}} \times$$

$$\left[\tan(\frac{\alpha}{2}) \ln\left(\frac{k^2 + 2qk\cos(\frac{\alpha}{2}) + q^2}{k^2 - 2qk\cos(\frac{\alpha}{2}) + q^2}\right) + 2\arctan\left(\frac{k^2 - q^2}{2qk\sin(\frac{\alpha}{2})}\right)\right] \tag{2.43}$$

with $q = (\tilde{m}^2(E^2 + \Gamma^2)/\hbar^4)^{\frac{1}{4}}$, $\cos\alpha = E/\sqrt{E^2 + \Gamma^2}$, and $\sin\alpha = \Gamma/\sqrt{E^2 + \Gamma^2}$.

2.4 Magnetic field in the (x-z) plane

We consider the gauge $\vec{A} = (-B_\perp y, 0, B_\parallel y)$ similar to ref.[15, 16], which gives a magnetic field in the (x-z) plane that makes an angle $\theta = \arctan(-B_\perp/B_\parallel)$ with the x axis. If the confining potential is harmonic, $m\Omega^2 y^2/2$, then the Schrödinger equation is

$$-\frac{\hbar^2}{2m}\frac{\partial^2\Psi}{\partial x^2} + -\frac{\hbar^2}{2m}\frac{\partial^2\Psi}{\partial y^2} + \frac{e^2B_\perp^2}{2m}y^2\Psi + \frac{e^2B_\parallel^2}{2m}y^2\Psi$$

$$+\frac{m}{2}\Omega^2 y^2\Psi - \frac{\imath e\hbar B_\perp y}{m}\frac{\partial\Psi}{\partial x} = \epsilon\Psi. \tag{2.44}$$

Assuming solutions of the form $\Psi(x,y) = \exp(\imath k_x x)\phi(y)$, Eq. (2.44) can be further simplified and put in the form

$$-\frac{\hbar^2}{2m}\frac{d^2\phi}{dy^2} + \frac{m\varpi^2}{2}\left[y + y_o\right]^2\phi = \left[\epsilon' - \frac{\hbar^2k_x^2}{2m} + \frac{\omega_\perp^2\hbar^2k_x^2}{2\varpi^2 m}\right]\phi \tag{2.45}$$

where, $\varpi = \omega^2 + \Omega^2$, $\omega^2 = \omega_\perp^2 + \omega_\parallel^2$, $\omega_\perp = eB_\perp/m$, and $\omega_\parallel = eB_\parallel/m$. The y_o term is $\tilde{b}\tilde{l}^2k_x$, with $\tilde{b} = \omega_\perp/\varpi$ and $\tilde{l}^2 = \hbar/m\varpi$. The solution to Eq. (2.45) is the wave function

$$\Psi_{n,k_x}(x,y) = \sqrt{\frac{1}{\tilde{l}L_x\sqrt{\pi}2^n n!}}H_n\left(\frac{y+\tilde{b}\tilde{l}^2k_x}{\tilde{l}}\right)\exp(\imath k_x x - \frac{(y+\tilde{b}\tilde{l}^2k_x)^2}{2\tilde{l}^2}). \tag{2.46}$$

The eigenvalue is

$$\epsilon = (n + \frac{1}{2})\hbar\varpi + \frac{\hbar^2 k_x^2}{2\tilde{m}} \tag{2.47}$$

and the effective mass $\tilde{m} = m/(1 - \tilde{b}^2)$.

2.4.1 Density of states

Following the steps used to determine the DOS for other orientations of the B-field, we find the DOS to be identical in form to that given by Eq. (2.22)

$$D(\epsilon) = \sqrt{\frac{\tilde{m}}{2\pi^2\hbar^2}} \sum_n \frac{1}{\sqrt{E}}. \tag{2.48}$$

2.5 Magnetic field in the (x-y) plane of a wire with finite thickness

We use the gauge $\vec{A} = (-B_+ z, B_{||} z, 0)$ [15, 16] so that the magnetic field is in the (x-y) plane and makes an angle $\theta = \arctan(B_+/B_{||})$ with the y axis. If we assume that the confining potential is harmonic in both the z and y directions, with $\Omega_z \gg \Omega_y$, then the Schrödinger equation becomes

$$-\frac{\hbar^2}{2m}\frac{\partial^2\Psi}{\partial x^2}+-\frac{\hbar^2}{2m}\frac{\partial^2\Psi}{\partial y^2}+-\frac{\hbar^2}{2m}\frac{\partial^2\Psi}{\partial z^2}+\frac{m}{2}\varpi^2 z^2\Psi$$

$$+\imath\hbar\omega_{+}z\frac{\partial\Psi}{\partial x}+-\imath\hbar\omega_{\|}z\frac{\partial\Psi}{\partial y}+\frac{m\Omega_y^2 y^2}{2}\Psi=\epsilon\Psi, \tag{2.49}$$

where, $\omega_{\|}=eB_{\|}/m$, $\omega_{+}=eB_{+}/m$,and $\varpi^2=\omega_{\|}^2+\omega_{+}^2+\Omega_z^2$. This equation is not separable. However, if we assume $B_{+}\gg B_{\|}$, then the $-\imath\hbar\omega_{\|}z\partial\Psi/\partial y$ term can be treated as a perturbation with the rest of the equation being separable. Assuming solutions of the form $\Psi=C\phi(y)Z(z)\exp(\imath k_x x)$, Eq. (2.49) results in two one-dimensional harmonic oscillators for the y and z variables and plane wave solutions in the x variable. The wave functions to the unperturbed problem are then

$$\Psi_{n,s,k_x}(x,y) = \sqrt{\frac{1}{\tilde{l}_n\tilde{l}_s L_x\sqrt{\pi}2^{n+s}s!n!}}H_n\left(\frac{z-\tilde{b}\tilde{l}_n^2k_x}{\tilde{l}_n}\right)H_s\left(\frac{y}{\tilde{l}_s}\right)$$

$$\exp\left(-\frac{(z-\tilde{b}\tilde{l}_n^2k_x)^2}{2\tilde{l}_n^2}-\frac{y^2}{2\tilde{l}_s^2}+\imath k_x x\right). \tag{2.50}$$

where, $\tilde{b}=\omega_{+}/\varpi$, $\tilde{l}_n^2=\hbar/m\varpi$ and $\tilde{l}_s=\hbar/m\Omega_y$. The eigenvalues are

$$\epsilon^{(0)}=(n+\frac{1}{2})\hbar\varpi+(s+\frac{1}{2})\hbar\Omega_y+\frac{\hbar^2k_x^2}{2\tilde{m}} \tag{2.51}$$

and the effective mass $\tilde{m}=m/(1-\tilde{b}^2)$

2.5.1 Perturbation theory

The perturbation term $\propto \partial\Psi/\partial y$ in Eq. (2.49) will not give any first order corrections (see [9, 10]) but can be treated using second-order perturbation theory. The energy correction is given by inserting this perturbation into Eq.(2.9), i.e.,

$$\epsilon^{(2)} = \hbar^2\omega_{||}^2 \sum_{n\neq s} \frac{\langle n, s, k_x|z\frac{\partial}{\partial y}|n', s', k_x'\rangle\langle n', s', k_x'|z\frac{\partial}{\partial y}|n, s, k_x\rangle}{E_{n,s,k_x} - E_{n',s',k_x'}} \tag{2.52}$$

Using the recursion relations and orthogonality properties of the Hermite polynomials, this formula can be simplified to give

$$\epsilon^{(2)} = \frac{\hbar\omega_{||}^2\Omega_y^2}{2\varpi^2}\left[\frac{s\varpi + n\omega_{||} - 2sn\omega_{||}}{\varpi^2 - \omega_{||}^2}\right]. \tag{2.53}$$

The total energy is the sum of Eqs. (2.51), and (2.53)

$$\epsilon = (n+\frac{1}{2})\hbar\varpi + (s+\frac{1}{2})\hbar\Omega_y + \frac{\hbar^2k_x^2}{2\bar{m}} + \epsilon^{(2)}. \tag{2.54}$$

2.5.2 Density of states

Using Eq. (2.20) for the DOS, we can derive the expression

$$D(\epsilon) = \sqrt{\frac{\bar{m}}{2\pi^2\hbar^2}} \sum_n \sum_s \frac{1}{\sqrt{\epsilon - \left(n+\frac{1}{2}\right)\hbar\varpi - (s+\frac{1}{2})\hbar\Omega_y - \epsilon^{(2)}}}. \tag{2.55}$$

2.6 Magnetic field in the (y-z) plane of a wire of finite thickness

We use the gauge $\vec{A} = (B_{\dagger}z - B_{\perp}y, 0, 0)$ [15, 16], which gives a magnetic field in the (y-z) plane that makes an angle $\theta = \arctan(B_{\dagger}/B_{\perp})$ with the z axis. Inserting this gauge into the Schrödinger equation along with a confining potential of the form $m[\Omega_y^2 y^2 + \Omega_z^2 z^2]/2$, where $\Omega_z \gg \Omega_y$, we have

$$-\frac{\hbar^2}{2m}\frac{\partial^2\Psi}{\partial x^2} + -\frac{\hbar^2}{2m}\frac{\partial^2\Psi}{\partial y^2} + -\frac{\hbar^2}{2m}\frac{\partial^2\Psi}{\partial z^2} + \frac{m}{2}\varpi^2 y^2\Psi +$$

$$+\frac{m}{2}\omega_z^2 z^2\Psi + \imath\hbar\omega_{\perp}y\frac{\partial\Psi}{\partial x} + -\imath\hbar\omega_{\dagger}z\frac{\partial\Psi}{\partial x} + \frac{m}{2}\omega_{\dagger}\omega_{\perp}zy\Psi = \epsilon\Psi. \qquad (2.56)$$

In this equation we have $\varpi = \Omega_y^2 + \omega_{\perp}^2$, $\omega_z = \Omega_z^2 + \omega_{\dagger}^2$, $\omega_{\perp} = eB_{\perp}/m$, and $\omega_{\dagger} = eB_{\dagger}/m$.

The cross term $m\omega_{\dagger}\omega_{\perp}zy/2$ in Eq. (2.56) is not separable. However, if we make the assumption $\omega_{\perp} \gg \omega_{\dagger}$, the non-separable term can be treated as a perturbation. The rest of the equation can be dealt with if we choose solutions of the form $C\phi(y)Z(z)\exp(\imath k_x x)$. As a result, we obtain equations for a harmonic oscillator in

y and z directions and plane-wave solutions in x. The wave function is of the form

$$\Psi_{n,s,k_x}(x,y) = \sqrt{\frac{1}{\tilde{l}\tilde{l}_z L_x \sqrt{\pi} 2^{n+s} s! n!}} H_n\left(\frac{y-\tilde{b}\tilde{l}^2 k_x}{\tilde{l}}\right) H_s\left(\frac{z+\tilde{b}_z \tilde{l}_z^2 k_x}{\tilde{l}_z}\right)$$

$$\times \exp\left(-\frac{(y-\tilde{b}\tilde{l}^2 k_x)^2}{2\tilde{l}^2} - \frac{(z+\tilde{b}_z \tilde{l}_z^2 k_x)^2}{2\tilde{l}_z^2} + \imath k_x x\right),$$

where $\tilde{b} = \omega_\perp/\varpi$, $\tilde{l}^2 = \frac{\hbar}{m\varpi}$, $\tilde{b}_z = \omega_+/\omega_z$, and $\tilde{l}_z = \hbar/m\omega_z$. The eigenvalues are

$$\epsilon = (n+\frac{1}{2})\hbar\varpi + (s+\frac{1}{2})\hbar\omega_+ + \frac{\hbar^2 k_x^2}{2\tilde{m}} \tag{2.57}$$

and the effective mass $\tilde{m} = m/(1+\tilde{b}^2-\tilde{b}_z^2)$.

2.6.1 Perturbation theory

The corrected eigenvalue is found using second-order perturbation theory. As in the previous sections the perturbation is an odd function of the z and y variables and so by the orthogonality of the Hermite polynomials the first-order correction is zero. Inserting the perturbation term $m\omega_\perp\omega_+ zy/2$ in Eq. (2.9) the correction is found to be

$$\epsilon^{(2)} = \frac{\hbar\omega_+^2\omega_\perp^2}{8\varpi\omega_z(\varpi^2-\omega_{||}^2)}\left[n\omega_z - m\varpi\right]. \tag{2.58}$$

The effect of a magnetic field tilted to the plane of the quantum wire was studied experimentally in ref. [13, 14], they showed that the motion of the electron is clearly affected by both components of the magnetic field. However, the results

they found were for large θ and so the results found in Eq. (2.56)-(2.58) are not applicable and the solution to Eq. (2.56) would have to be found numerically.

2.6.2 Density of states

Using Eq. (2.20) we obtain the DOS as

$$D(\epsilon) = \sqrt{\frac{\tilde{m}}{2\pi^2\hbar^2}} \sum_n \sum_m \frac{1}{\sqrt{\epsilon - \left(n+\frac{1}{2}\right)\hbar\varpi - \left(m+\frac{1}{2}\right)\hbar\omega_+ - \epsilon^{(2)}}}. \tag{2.59}$$

2.7 Discussion

The Schrödinger equation has been solved for six different orientations of the magnetic field. The confining potential was chosen to be harmonic in all cases with anharmonic terms evaluated only when the magnetic field is perpendicular or parallel to the plane of the wire. The reason is, that for all other orientations of the magnetic field the energy eigenvalues are not as simple to evaluate. In most cases, other subbands are introduced (whenever the wire has a finite thickness) further complicating the application of perturbation theory when the anharmonic terms are added. Furthermore, when the magnetic field makes an angle with respect to one of the major axes, the Schrödinger equation is not always separable. If, however, one of the components of the magnetic field is far greater than the other we may apply perturbation theory. Also, when the tilt of the magnetic field is taken

to be very small, the solutions are very similar to those for which the magnetic field is along one of the major axes.

The eigenvalues are used to determine the DOS of the quantum wire. By comparing the DOS for the different confinement potentials we are able to determine what effect these extra terms will have on the Fermi level. The graphs, Fig. 2.3 and 2.6 of the different DOS show very little difference between them and so the Fermi level can also be assumed to change very little with the addition of the small anharmonic terms.

Chapter 3

d.c. Conductivity tensor

3.1 Kubo-Greenwood formulas

In the one electron approximation the d.c. conductivity tensor can be obtained from the Kubo-Greenwood formulas [17, 21]. These formulas relate the one-electron energy and wave function to the conductivity tensor, by treating electron collisions with impurities and phonons as small perturbations. In a given representation the density operator has a "diagonal" and "non-diagonal" contribution. The corresponding diagonal contribution to the conductivity can be written [19] as the sum of a diffusion term

$$\sigma_{\mu\nu}(0) = \frac{\beta e^2}{V} \sum_{\xi} f_\xi (1 - f_\xi) \tau(\epsilon_\xi) v_\mu^\xi v_\nu^\xi, \tag{3.1}$$

and a collision term

$$\sigma_{\mu\mu}(0) = \frac{\beta e^2}{2V} \sum_{\xi} \sum_{\xi'} f_{\xi}(1 - f_{\xi'}) W_{\xi\xi'} (\alpha_{\mu}^{\xi} - \alpha_{\mu}^{\xi'})^2. \tag{3.2}$$

Here,$|\xi\rangle$ is the eigenstate,$\beta = 1/k_B T$, $v_{\mu}^{\xi} = \langle \xi | v_{\mu} | \xi \rangle$ is the expectation value of the velocity operator in the μ direction, V the volume of the sample, ϵ_{ξ} the one electron energy and $\alpha_{\mu}^{\xi} = \langle \xi | \alpha_{\mu} | \xi \rangle$ is the expectation value of the position operator of the electron. The relaxation time τ is given by

$$\frac{1}{\tau(E_{\xi})} = \sum_{\xi} W_{\xi\xi'}, \tag{3.3}$$

and $W_{\xi\xi'}$ is the transition matrix given by Fermi's golden rule [9]

$$W_{\xi\xi'} = \frac{2\pi N_i}{\hbar V} \sum_{q} |U(q)|^2 |\langle \xi | \exp(i\vec{q} \cdot \vec{r}) | \xi' \rangle|^2 \delta(\epsilon_{\xi} - \epsilon_{\xi'}); \tag{3.4}$$

N_i is the concentration of the impurities and $U(\vec{q})$ the Fourier transform of the impurity potential.

The nondiagonal contribution of the conductivity [19] makes explicit use of the nondiagonal velocity elements. In this case $\langle \xi' | v_{\mu} | \xi \rangle = 0$ and so there is no contribution from $\sigma_{xx}^{nd}(0)$ to the total conductivity tensor.

3.1.1 Impurity Scattering

At low temperature impurity scattering dominates the conductivity of the quantum wire and we model its effect using three different potentials [20]. One choice

is the Gaussian potential

$$V(\vec{r}) = \frac{V_o}{\pi d^2} \exp(-\frac{r^2}{d^2}), \tag{3.5}$$

where V_o is a constant, proportional to its strength, and d is its effective range. Another choice is the Dirac $\delta-$function potential

$$V(\vec{r}) = V\delta(\vec{r}), \tag{3.6}$$

which would model the extreme case of the Gaussian potential ($d \to 0$), where the electron is scattered "suddenly" by a neutral impurity. Finally, we use the screened Coulomb potential,

$$V(\vec{r}) = \frac{e^2 \exp(-k_s|\vec{r}|)}{\epsilon|\vec{r}|}, \tag{3.7}$$

to model the scattering of an electron by a charged impurity. The effect of these potentials is evaluated using the Golden rule Eq. (3.4), which makes use of the Fourier transform of the potentials. The transform of Eq. (3.5) is

$$U(q) = \frac{V_o}{2\pi} \exp(-\frac{q_\perp^2 d^2}{4}), \tag{3.8}$$

with $q_\perp^2 = q_x^2 + q_y^2$. The transform of the $\delta-$function and screened-Coulomb potential are, respectively,

$$U(\vec{q}) = \frac{V}{\sqrt{2\pi}} \tag{3.9}$$

and

$$U(\vec{q}) = 2\pi e^2 \sqrt{\frac{q_\perp^2 + k_s^2}{\epsilon}}. \tag{3.10}$$

3.1.2 Phonon Scattering

The transition matrix $W_{\xi\xi'}$ [17, 20, 24] for electron- phonon scattering is

$$W_{\xi\xi'} = \sum_q [Q^+ N_o + Q^-(1 + N_o)], \tag{3.11}$$

where

$$Q^{\pm} = \frac{2\pi}{\hbar}|F(q)|^2 |\langle \xi'| \exp(\pm i\vec{q}\cdot\vec{r})|\xi\rangle|\delta(E_\xi - E_{\xi'} \pm \hbar\omega_q). \tag{3.12}$$

Here $F(q)$ is the Fourier transform of the electron- phonon interaction, ω_q the phonon frequency, and N_o the average number of phonons. Two interactions are assumed to dominate, acoustic phonons at low temperatures and optical phonons at high temperatures. The interaction potential for the acoustic phonons [20] is,

$$|F(\vec{q})|^2 = \frac{c^2}{2V_o \rho u_o} q, \tag{3.13}$$

with ρ being the density of the material, u_o the velocity of sound in it, and c a constant. For the purpose of simplifying the calculations, we make the approximation $q \approx q_\perp = \sqrt{q_x^2 + q_y^2}$.

Optical phonons [20] are modeled with the interaction

$$|F(\vec{q})|^2 = \frac{\hbar^2 D^2}{V_o \rho E} = \frac{D'}{V_o}, \tag{3.14}$$

where $E = \hbar\omega_L$ and D is a constant.

3.2 Magnetic field perpendicular to the wire

3.2.1 Matrix elements

When evaluating the conductivity tensor, given by Eq. (3.1) or Eq. (3.2), we use the matrix elements $|\langle nk|\exp(i\vec{q}\cdot\vec{r})|n'k'\rangle|^2$. This integral can be solved for the unperturbed wave function given in Eq. (2.4) and the result is [12]

$$|\langle nk|\exp(i\vec{q}\cdot\vec{r})|n'k'\rangle|^2 = \frac{n'!}{n!}u^{n'-n}e^{-u}|L_{n'}^{n'-n}(u)|^2\delta_{k',k-q_x} = |J_{nn'}(u)|^2\delta_{k',k-q_x}, \quad (3.15)$$

with $u = l^2(b^2q_x^2 + q_y^2)/2$ and $L_{n'}^{n'-n}(u)$ the Laguerre polynomial.The same wave function is used to find the expectation values for the position and velocity operators

$$\langle nk|\alpha_x|nk\rangle = 0, \qquad \langle nk|\alpha_y|nk\rangle = bl^2k_x \quad (3.16)$$

$$\langle nk|v_x|nk\rangle = \frac{\hbar k_x}{\tilde{m}}, \qquad \langle nk|v_y|nk\rangle = 0. \quad (3.17)$$

3.2.2 Conductivity tensor for impurity scattering

Gaussian potential

Before the conductivity tensors can be determined, the relaxation time τ and the transition probability $W_{\xi\xi'}$ from state ξ' to state ξ must be calculated. Inserting the matrix elements (3.15) - (3.17) into Eq. (3.4) and considering a two-dimensional

sample of area A we obtain

$$W_{\xi\xi'} = \frac{2\pi N_i}{\hbar A} \sum_q |J_{nn'}(u)|^2 \delta_{k',k-q_x} \delta(\epsilon_\xi - \epsilon_{\xi'}). \tag{3.18}$$

Using this result in Eq. (3.3) we obtain

$$\frac{1}{\tau} = \frac{N_i V_o^2}{2\pi\hbar A} \sum_{n'k'_x} \sum_q \exp(-q_\perp^2 d^2/4) |J_{nn'}(u)|^2 \delta_{k',k-q_x} \delta(\epsilon_\xi - \epsilon_{\xi'}). \tag{3.19}$$

When considering elastic scattering by impurities we assume that there is no transitions between different Landau levels so that, $n' \to n$ and $|J_{nn'}(u)|^2 \to |J_{nn}(u)|^2 = \exp(-u)|L_n(u)|^2$. In order to simplify Eq. (3.19), the two sums can be converted into integrals $\sum_{k'_x} = L_x \int dk'_x/2\pi$ and $\sum_q = A \int\int dq_x dq_y/4\pi^2$. The δ function can be expanded in terms of q_x to give $\tilde{m}[\delta(q_x - 2k_x) + \delta(q_x)]/k_x\hbar^2$. We can then write Eq. (3.19) in the form

$$\frac{1}{\tau} = \frac{\tilde{m} N_i V_o^2 L_x}{8\pi^3\hbar^3 k_x} \int dq_y \exp(-q_y^2 d^2/2) \left[|J(0,q_y)|^2 + \exp(-2k_x^2 d^2)|J(k_x,q_y)|^2\right]. \tag{3.20}$$

Inserting the inverse of Eq. (3.20) into Eq. (3.1) gives the diffusion term's contribution to the conductivity as

$$\sigma_{xx} = \frac{8\pi^3\hbar^3 e^2 \beta}{\tilde{m} N_i V_o^2 L_x}$$

$$\times \sum_{n,k_x} \frac{f_{nk_x}(1 - f_{nk_x}) k_x (\frac{\hbar k_x}{\tilde{m}})^2}{\int \exp(-q_y^2 d^2/2)[|J(0,q_y)|^2 + \exp(-2k_x^2 d^2)|J(k_x,q_y)|^2] dq_y} \tag{3.21}$$

Also, because $\langle nk|v_y|nk\rangle = 0$ we have

$$\sigma_{yy} = \sigma_{xy} = \sigma_{yx} = 0. \tag{3.22}$$

Since impurity scattering dominates at low temperatures the expression for σ_{xx} can be further simplified with the relation $\beta f_{nk_x}(1 - f_{nk_x}) \longrightarrow \delta(\epsilon_{n,k_x} - \epsilon_F)$ as $T \longrightarrow 0$. The diffusion term of the conductivity can be written in the form

$$\sigma_{xx} = \frac{2\pi^2\hbar^5 e^2}{\tilde{m}^3 N_i V_o^2 A}$$

$$\times \sum_n \int \frac{\delta(\epsilon_{n,k_x} - \epsilon_f) k_x^3 dk_x}{\int \exp(-q_y^2 d^2/2)[|J(0,q_y)|^2 + \exp(-2k_x^2 d^2)|J(k_x,q_y)|^2] dq_y}. \tag{3.23}$$

Making use of the substitution $v = \hbar^2 k_x^2/2\tilde{m}$, the integral over k_x states can be evaluated to give

$$\sigma_{xx}(0) = \frac{4\pi^2 e^2 \hbar}{\tilde{m} N_i V_o^2 A} \sum_n \frac{E}{I_1(E, q_y)}. \tag{3.24}$$

This gives the conductivity as a function of $E = \epsilon_f - (n + \frac{1}{2})\hbar\varpi$; as a result σ_{xx} is a function of the magnetic field B. The function $I_1(E, q_y)$ must be evaluated numerically and is given by

$$I_1(E, q_y) = \int dq_y \exp(-\frac{a^2 u}{l^2}) \left[|L_n(u)|^2 + K|L_n(\frac{2\tilde{m}b^2 l^2 E}{\hbar^2} + u)|^2 \right], \tag{3.25}$$

with $u = l^2 q_y^2/2$, $K = \exp(-4r^2 E\tilde{m}/\hbar^2)$, $a^2 = d^2 + l^2$, and $r^2 = d^2 + b^2 l^2/2$.

In Fig. 3.1, we have plotted Eq. (3.24) as a function of the magnetic field. It is evident from the form of the graph that the dominant term in the expression is $(1 - b^2) = 1 - (\omega_c/\varpi)^2$ when the magnetic field is above 1 Tesla. However, below 1 Tesla the dominant term will be the the integral $I_1(E, q_y)$, specifically the Laguerre polynomials which will increase with an increasing magnetic field. This leads to the peak in Fig. 3.1. Essentially, what is happening is that at small magnetic fields, the diffusion term will increase because the electrons will travel fairly unhindered through the wire. As the magnetic field increases so does the cyclotron frequency and as a consequence it becomes equal to or greater than the harmonic confinement Ω of the wire and so does not travel as easily through it.

The confining potential enters the expression only through the Fermi level and the matrix elements (3.15) - (3.17). As a result, the addition of small higher order terms into the confining potential will not have any appreciable effect on the conductivity.

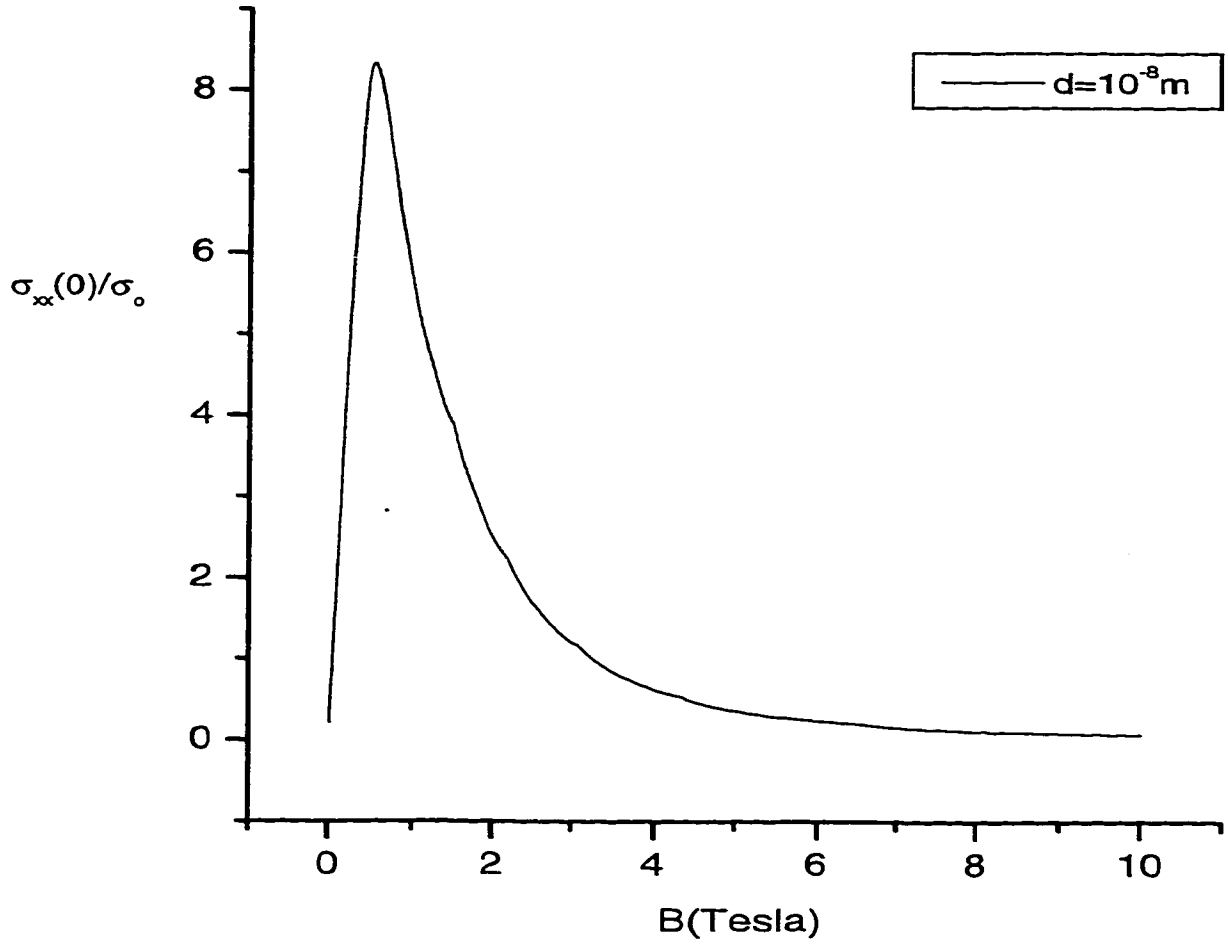

Figure 3.1: Diffusion term of the conductivity as a function of the magnetic field. The scattering potential is Gaussian and $\sigma_o = 10^7 m N_i V_o^2 L_x / 4\pi^2 \hbar L_y$.

The contribution of the collision term is given by Eq. (3.2). Following the same procedure as we did for the diffusion term and assuming that all collisions are elastic, we have for Eq. (3.2)

$$\sigma_{xx} = \frac{\beta e^2 \tilde{m} N_i V_o^2 L_x}{4\pi^3 \hbar^3 A_o} \sum_{nk} f_{nk}(1 - f_{nk})$$

$$\times \int dq_y \exp(-2k_x^2 d^2 - \frac{q_y^2 d^2}{2}) |J(k_x, q_y)|^2 (bl^2)^2 k_x. \tag{3.26}$$

In order, to further simplify the expression we once again work with the low temperature limit and convert the sum over k_x into an integral. The integration can then be carried out by substituting $v = \hbar^2 k_x^2 / 2\tilde{m}$. This gives

$$\sigma_{xx} = \frac{e^2 \tilde{m}^2 N_i V_o^2 L_x^2 (bl^2)^2}{8\pi^4 \hbar^5 A_o} \sum_{n} I_2(E, q_y) \tag{3.27}$$

with the function I_2 given by the integral

$$I_2(E, q_y) = \exp(-\frac{4\tilde{m} E r^2}{\hbar^2}) \int dq_y \exp(-a^2 q_y^2/2) |L_n^o(l^2(\frac{2\tilde{m} E b^2}{\hbar^2} + q_y^2/2))|^2 \tag{3.28}$$

Eq. (3.27) is plotted as a function of the magnetic field in Fig. (3.2). The dominant term is the function $I_2(E, q_y)$ it determines where the peaks will take place. This comes about because of the oscillatory nature of the Fermi level Fig. 3.3, when the magnetic field is perpendicular to the quantum wire. As the Fermi level increases, the integral I_2 will decrease, when the Fermi level decreases, I_2 will

increase. The magnitude of the peaks will be a result of the magnetic field term $(bl^2)^2/(1-b^2)$ and $I_2(E, q_y)$.

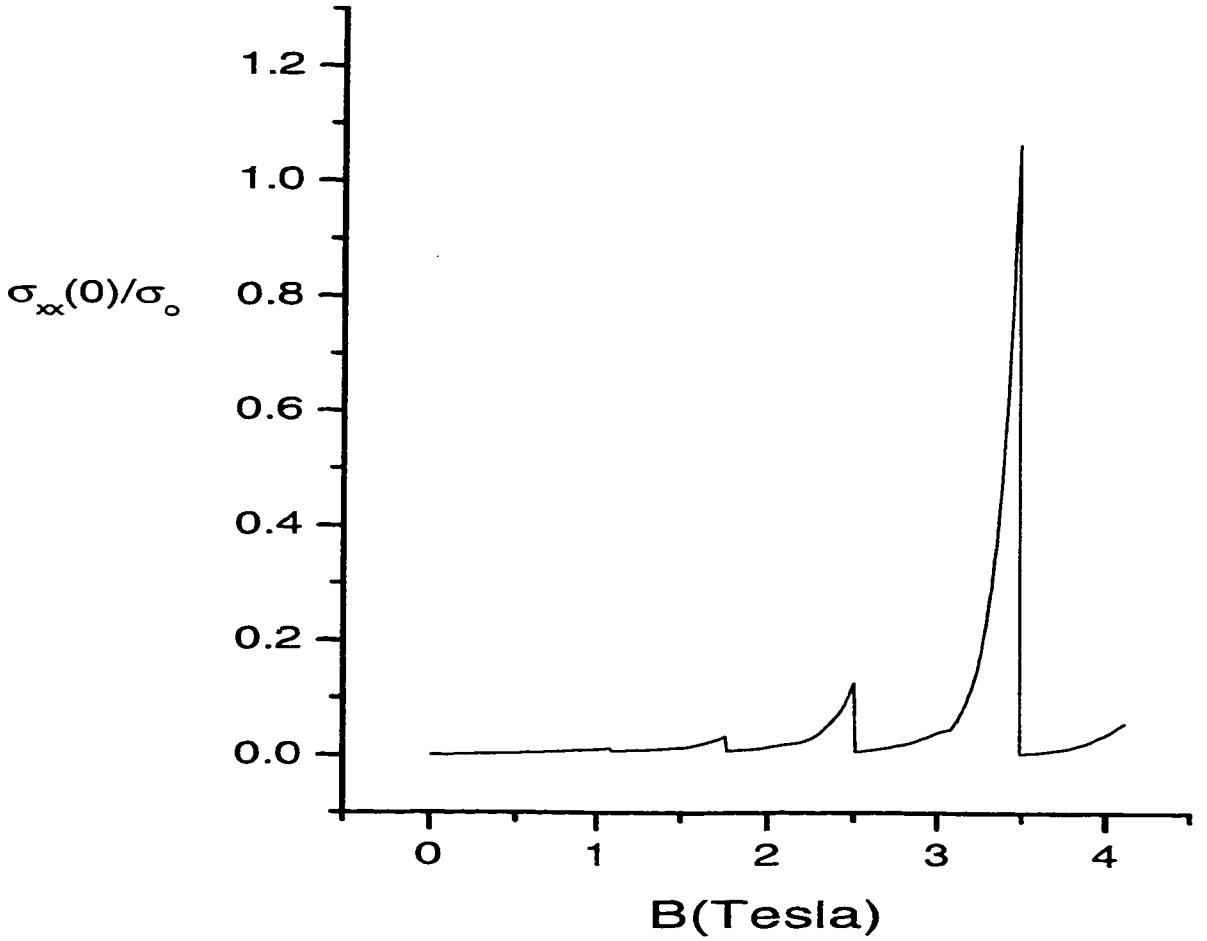

Figure 3.2: Collision term of the conductivity as a function of the magnetic field. The scattering potential is Gaussian and $\sigma_o = 8\pi^4\hbar/e^2m^2N_iV_o^2L_xL_y$.

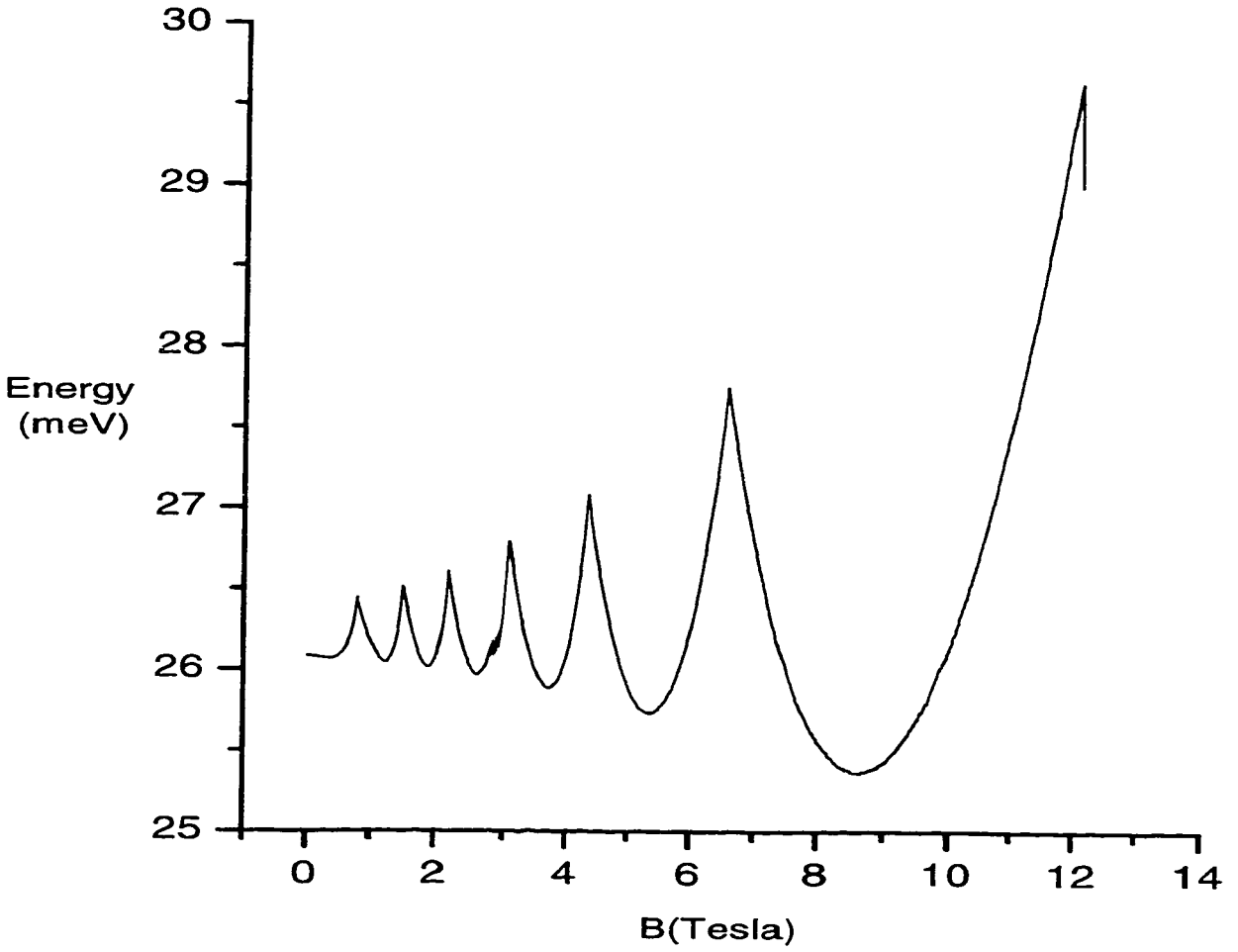

Figure 3.3: Fermi level as a function of the magnetic field.

δ-function potential

The δ function potential models a very short-range interaction between the electron and an electrically neutral impurity in the sample. Essentially the $\delta-$function scattering is identical to the Gaussian when $d \longrightarrow 0$ in Eq.(3.8). In order to determine the conductivity of the wire we follow the same procedure that was used for Gaussian scattering. We insert the Fourier transform of the $\delta-$function Eq. (3.8)into Eq. (3.4), and the matrix elements (3.15) - (3.17) to obtain expression,

$$W_{\xi\xi'} = \frac{2\pi N_i}{\hbar A_o} \sum_q \frac{V^2}{2\pi} |J_{nn'}(u)|^2 \delta_{k',k-q_x} \delta(\epsilon_\xi - \epsilon_{\xi'}). \tag{3.29}$$

The diffusion term of the conductivity is given by Eq. (3.1). The relaxation time τ is found from Eq. (3.3) after inserting the interaction term Eq. (3.9) of the δ function into the expression for W_{n,k_x,n',k'_x} above. We assume there is only elastic scattering so $n' \rightarrow n$ and convert the sum over q_x and k'_x into integrals. These inegrals can be evaluated by expanding the δ function to give $\delta(\epsilon_{n,k_x} - \epsilon) = \tilde{m}[\delta(q_x - 2k_x) - \delta(q_x)]/\hbar^2 k_x$. The relaxation time is

$$\frac{1}{\tau} = \frac{N_i V^2 L_x \tilde{m}}{8\pi^3 \hbar^3 k_x} \sum_n \int dq_y \left[|J(\frac{\tilde{l}^2}{2}(4bk_x^2 + q_y^2))|^2 + |J(\frac{\tilde{l}^2 q_y^2}{2})|^2 \right]. \tag{3.30}$$

Substituting the above expression for the relaxation time into Eq.(3.1) and using the low-temperature limit with the substitution $v = \hbar^2 k_x^2 / 2\tilde{m}$ gives the

diffusion term in the form

$$\sigma_{xx} = \frac{8\pi^2 e^2 \hbar}{N_i V^2 \tilde{m} A_o} \sum_n \frac{E}{I_3(q_y)}. \tag{3.31}$$

The function $I_3(E, q_y)$ in the denominator is given by the integral

$$I_3(E, q_y) = \int dq_y [|J(\frac{\tilde{l}^2}{2}(\frac{8bE\tilde{m}}{\hbar^2} + q_y^2))|^2 + |J(\frac{\tilde{l}^2 q_y^2}{2})|^2] \tag{3.32}$$

and $E = \epsilon_f - (n + 1/2)\hbar\varpi$.

In Fig. 3.4 we have plotted Eq. (3.31) as a function of the magnetic field. The graph is identical in form to Fig. 3.1 with $(1 - b^2)$ once again being the dominant term when $B > 1$ Tesla and the peak a result of the same mechanism as was described earlier.

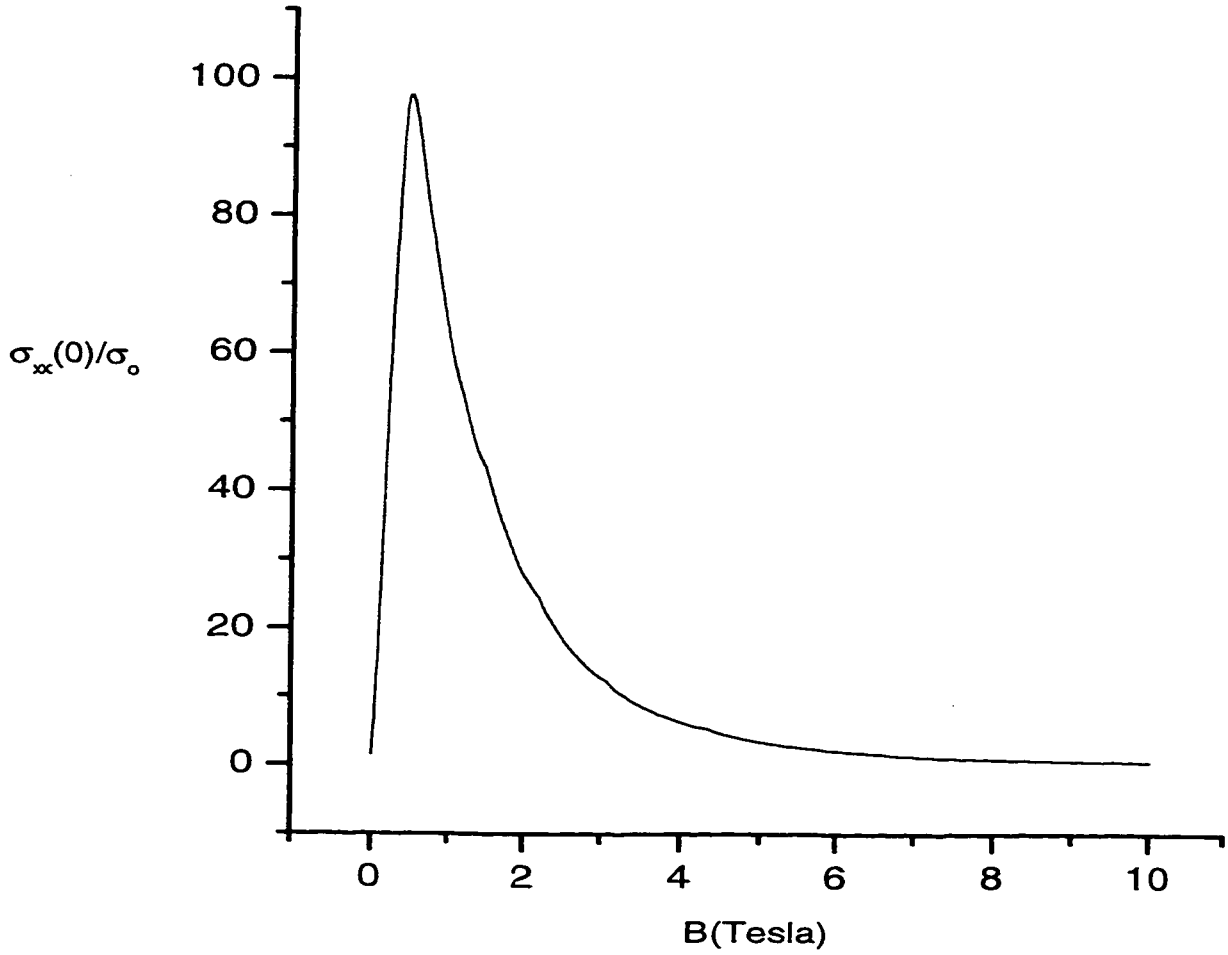

Figure 3.4: Diffusion term of the conductivity as a function of the magnetic field. The scattering potential is a $\delta-$function, $\sigma_o = 10^5 m N_i V_o^2 A/4\pi^2\hbar$.

The collision term can be found by inserting Eq. (3.29) into Eq. (3.2) to give,

$$\sigma_{xx} = \frac{\beta e^2 N_i V^2}{2A_o^2 \hbar} \sum_{n,k_x} \sum_{n',k_x'} \sum_{q} |J_{nn'}(u)|^2 \delta_{k_x', k_x - q_x} \delta(\epsilon - \epsilon')(b\tilde{l}^2)^2 (k_x - k_x')^2. \quad (3.33)$$

Integrating expression (3.33) over both q_x and k_x' gives

$$\begin{aligned} \sigma_{xx} &= \frac{\beta e^2 N_i V^2 (b\tilde{l}^2)^2 L_x \tilde{m}}{4\pi^3 A_o \hbar^3} \\ &\times \sum_{n,k_x} \int f_{n,k_x}(1 - f_{n,k_x}) |J_n(\frac{\tilde{l}^2}{2}(\frac{4\tilde{m}bk_x^2}{hbar^2} + q_y^2)|^2 k_x dq_y. \end{aligned} \quad (3.34)$$

Using the low-temperature limit and integrating over k_x we obtain the collision as

$$\sigma_{xx} = \frac{e^2 N_i V^2 (b\tilde{l}^2)^2 L_x \tilde{m}^2}{8\pi^4 L_y \hbar^5} \sum_{n} I_4(E, q_y). \quad (3.35)$$

The function $I_4(E, q_y)$ is an integral of the form

$$I_4(E, q_y) = \int dq_y |J_n(\frac{\tilde{l}^2}{2}(\frac{8\tilde{m}^2 bE}{\hbar^3} + q_y^2))|^2. \quad (3.36)$$

Eq. (3.35) is plotted in Fig. 3.5 again the form is identical to that of Fig. 3.2 with the integral determining where the peaks will take place and essentially for the same reasons.

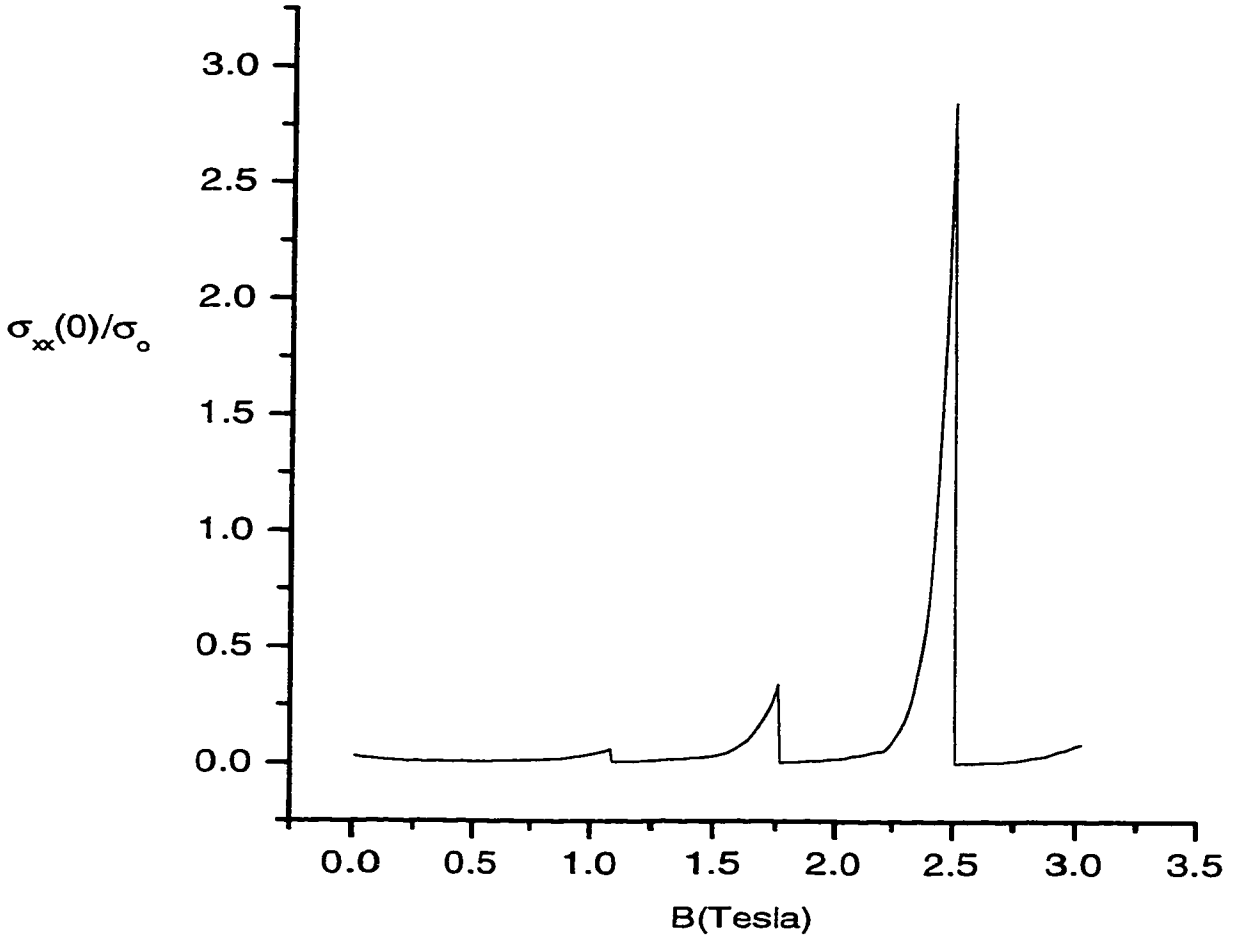

Figure 3.5: Collision term of the conductivity as a function of the magnetic field. The scattering potential is a $\delta-$ function one and $\sigma_o = 10^{-3} 8\pi^4 \hbar^5 L_y / m^2 N_i V_o^2 L_x$.

Screened Coulomb scattering

The conductivity tensor for the screened Coulomb potential is found using the same methods that were used to determine the conductivity of the Gaussian and $\delta-$ function potentials above. Once again we make use of the low-temperature limit and the elastic scattering approximation. For the diffusion term we obtain

$$\sigma_{xx} = \frac{\hbar\epsilon}{\pi N_i e^2 \tilde{m} A_o} \sum_n \frac{E}{I_5(E, q_y)}$$

where, $u = 8\tilde{m}E/\hbar^2$. The function $I_5(q_y)$ is given by the integral

$$I_5(q_y) = \int dq_y [u + q_y^2 + k_s^2] |J_n(\frac{\tilde{l}^2}{2}(ub^2 + q_y^2))|^2 + (q_y^2 + k_s^2)|J_n(\frac{\tilde{l}^2 q_y^2}{2})|^2 \qquad (3.37)$$

The presence of the inverse screening length k_s will act to widen the curve in Fig. 3.6. However, the dominant term is still the magnetic field term $1 - b^2$ with the confining potential having a small effect on the result of Eq. (3.37).

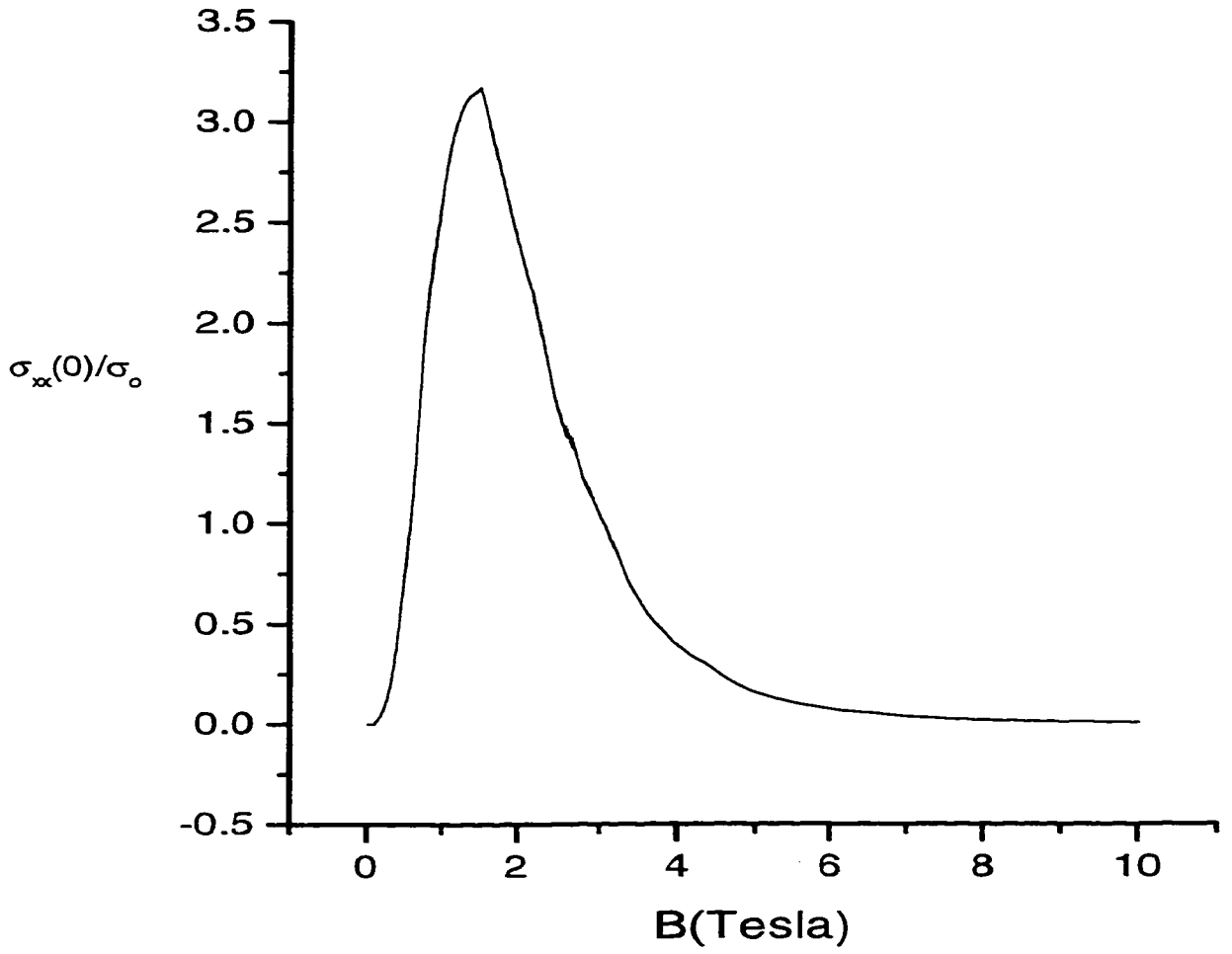

Figure 3.6: Diffusion term of the conductivity as a function of the magnetic field. The scattering potential is the screened Coulomb potential and $\sigma_o = 10_7 \pi m N_i A/\hbar\epsilon$.

The collision term is found to be

$$\sigma_{xx} = \frac{e^6 N_i (b\tilde{l}^2)^2 \tilde{m}^2 L_x}{\pi \epsilon L_y \hbar^5} \sum_n I_6(E, q_y) \tag{3.38}$$

with

$$I_6(E, q_y) = \int dq_y [\frac{8\tilde{m}E}{\hbar^2} + q_y^2 + k_s^2] |J_n(\frac{\tilde{l}^2}{2}(\frac{8b^2\tilde{m}E}{\hbar^2} + q_y^2)|^2. \tag{3.39}$$

In Fig. 3.7 we have plotted the collision term of Eq. (3.38) as function of the magnetic field. The form of the graph is essentially identical to the previous graphs of the collision term. There is however, a small difference due to the presence of k_s.

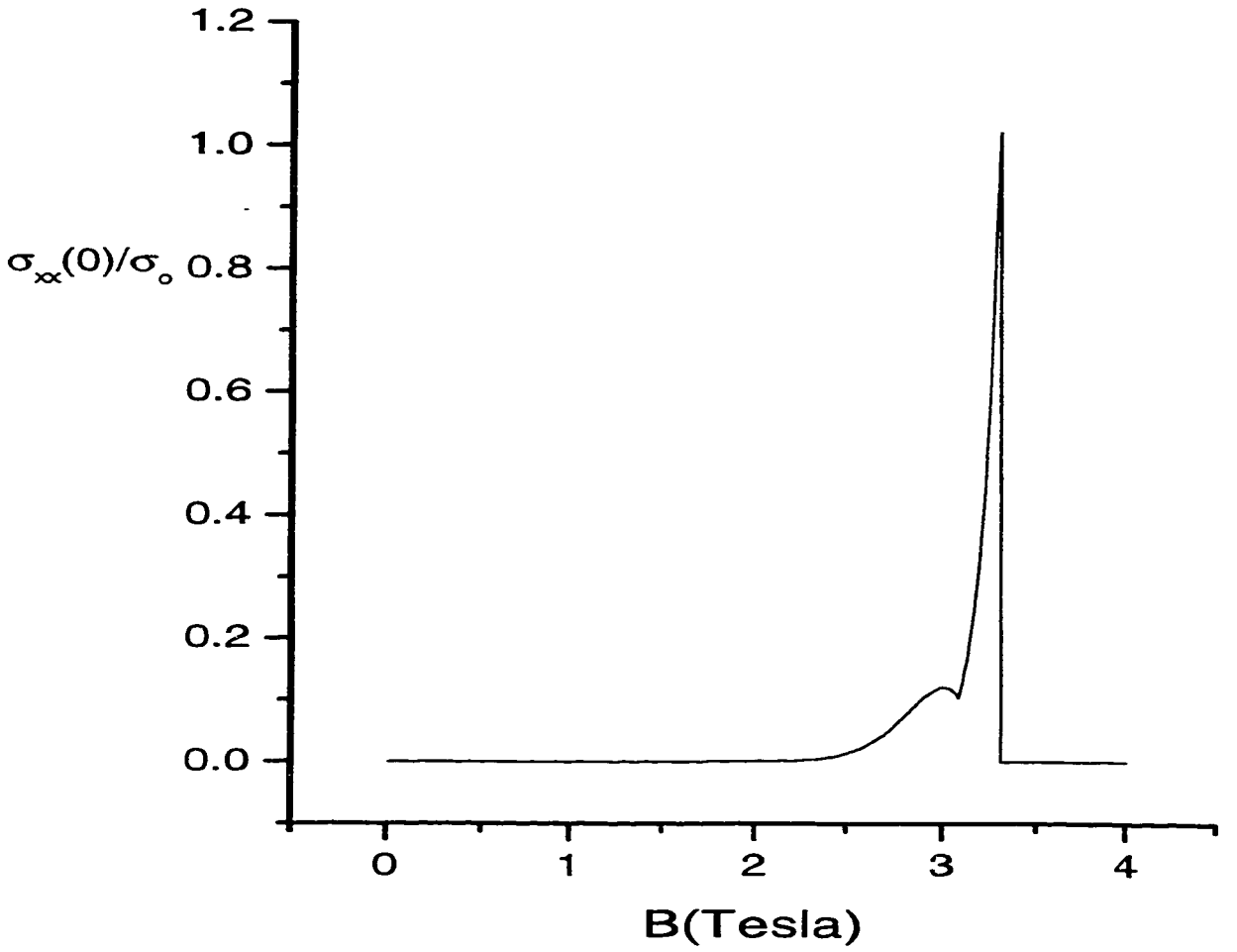

Figure 3.7: Collision term of the conductivity as a function of the magnetic field. The scattering potential is the screened Coulomb potential and $\sigma_o = 10^{-7}\pi m^2 e^6 N_i L_x/\hbar^5 L_y$.

3.2.3 Conductivity tensor for phonon scattering

Given the matrix elements for a magnetic field perpendicular to the wire (3.15)-(3.17), the transition matrix Eq. (3.4) can be put into the form

$$W_{\xi\xi'} = \frac{2\pi}{\hbar}\sum_{n',k_x'}|F(q)|^2|J(u)|^2\delta_{k_x',k_x-q_x}$$

$$\times\sum_{q}[\delta(E_\xi - E_{\xi'} + \hbar\omega_q)N_o + \delta(E_\xi - E_{\xi'} - \hbar\omega_q)(1+N_o)], \qquad (3.40)$$

where $u = \frac{l^2}{2}(bq_x^2 + q_y^2)$.

The collision term can be found by inserting Eq. (3.40) into Eq. (3.2) of the conductivity tensor and converting the sum over k_x' into an integral. Writing the δ function in the form $\delta[(n-n')\hbar\varpi + \frac{\hbar^2}{2\tilde{m}}[2k_xq_x - q_x^2] \pm \hbar\omega_q]$ it can ge further simplified by expanding it in a Taylor series about $q_x = 0$. All odd terms in the expansion vanish and the conductivity becomes

$$\sigma_{xx}(0) = \frac{\beta e^2(bl^2)^2}{4\pi\hbar^2 L_y\varpi}\sum_{n,k_x,m,q} f_{n,k_x}|F(q)|^2q_x^2\delta(m-\Delta) \qquad (3.41)$$

$$\times\left[|J_{n+m,n}(u)|^2(1-f_{n+m,k_x-q_x})N_o + (1-f_{n-m,k_x-q_x})|J_{n-m,n}(u)|^2(1+N_o)\right]$$

where, $n'-n = m$ for phonon absorption and $n'-n = -m$ for phonon emission, and $\Delta = \omega_q/\varpi$. The above expression can be simplified using Poisson's summation

formula [18, 23]

$$\sum_{m=0}^{\infty} g(m+\frac{1}{2}) = \int_0^{\infty} g(x)dx + 2\sum_{s=1}^{\infty}(-1)^s \int g(x)\cos(2\pi sx)dx. \tag{3.42}$$

As a result, we can write σ_{xx}^{coll} in the form

$$\sigma_{xx}(0) = \frac{C(bl^2)^2}{\varpi} \sum_{n,k_x,q} f_{n,k_x}|F(q)|^2 q_x^2 \left[1 + 2\sum_{s=1}^{\infty}(-1)^s \cos(2\pi s\Delta)\right]$$

$$\times \left[|J_{n\pm\Delta,n}(u)|^2(1 - f_{n\pm\Delta,k_x-q_x})N_o\right] \tag{3.43}$$

where $C = \beta e^2/4\pi\hbar^2 L_y$ and $(1 + N_o) \approx N_o$.

The diffusion term of the conductivity tensor is given by Eq. (3.1), the relaxation time τ is found in much the same way as the conductivity tensor is found for the collision term. The δ function is expanded in a Taylor series and the only surviving term would be $\delta(n' - n \pm \Delta)$. By transforming the sums into integrals the relaxation time becomes

$$\frac{1}{\tau} = \frac{L_x}{\hbar^2\varpi} \sum_q |F(q)|^2 \left[1 + 2\sum_s (-1)^s \cos(2\pi s\Delta)\right]$$

$$\times \left[N_o|J_{n+\Delta}(u)|^2 + (1 + N_o)|J_{n-\Delta}(u)|^2\right] \tag{3.44}$$

Inserting the relaxation time along with the matrix elements into the diffusion term gives

$$\sigma_{xx} = \frac{\beta e^2 \hbar^4 \varpi}{2\pi \tilde{m}^2 A_o} \sum_n \int dk_x \frac{1}{[1 + 2\sum_s (-1)^s \cos(2\pi s\Delta)]} \tag{3.45}$$

$$\times \frac{f_{n,k_x}(1 - f_{n,k_x})k_x^2}{\sum_q |F(q)|^2 [|J_{n\pm\Delta}(u)|^2 N_o]} \tag{3.46}$$

Acoustic phonons at low temperatures

In the case of acoustic phonons the interaction potential is given by Eq. (3.13) and we can make the assumption $N_o \approx 1/\hbar u_o q_\perp$, with u_o being the speed of sound. The phonon energy is small compared to the electron energy at low temperature and so Δ is also small. This makes it possible to write $\beta f_{n,k_x}(1 - f_{n\pm\Delta,k_x-q_x})$ as $(1 \pm \Delta)\delta(\epsilon_n(k_x) - \epsilon_F)$,by expanding $(1 - f_{n\pm\Delta,k_x-q_x})$ in a Taylor series and neglecting second or higher order terms. Placing the above result into Eq. (3.43) and integrating over k_x gives

$$\sigma_{xx} = \frac{C'\alpha L_x (bl^2)^2}{8\pi^3 \hbar u_o} \sum_n \left[1 + 2\sum_{s=1}^{\infty} (-1)^s \cos(2\pi s\Delta)\right] \sqrt{\frac{2\tilde{m}E}{\hbar^2}} I_7(u), \tag{3.47}$$

with

$$I_7(u) = \int dq_x dq_y q_x^2 |J_{n\pm\Delta}(u)|^2 (1 \pm \Delta) \tag{3.48}$$

and $C' = C/\beta$ and $E = \epsilon_F - (n + \frac{1}{2})\hbar\varpi$.

The diffusion term Eq.(3.46) can be further simplified by using the low temperature limit $\beta f_{nk_z}(1 - f_{nk_z}) \longrightarrow \delta(\epsilon_{n,k_x} - \epsilon_F)$ and then integrating over k_x states

to give

$$\sigma_{xx} = \frac{e^2\hbar^2 u_o \varpi}{\sqrt{2\tilde{m}}\alpha\pi} \sum_{n,k_x} \frac{\sqrt{E}}{\left[1 + 2\sum_s (-1)^s \cos(2\pi s\Delta)\right] I_8(u)} \tag{3.49}$$

with

$$I_8(u) = \frac{1}{\int dq_x dq_y |J_{n\pm\Delta}(u)|^2}. \tag{3.50}$$

Optical phonons at high temperature

At high temperatures, the Fermi distribution can be converted to the Maxwell distribution and inserting the Eq. (3.14) into Eq.(3.43) we obtain for the collision term

$$\sigma_{xx} = \frac{C'D'}{\hbar u_o A_o^2} \sum_{n,k_x,q} \frac{q_x^2}{q_\perp} \left[1 + 2\sum_{s=1}^{\infty} (-1)^s \cos(2\pi s\Delta)\right]$$

$$\times \exp(-\beta(\epsilon_{n,k_x} - \epsilon_F)) \left[|J_{n+\Delta}(u)|^2 + |J_{n-\Delta}(u)|^2)\right]. \tag{3.51}$$

The expression for the diffusion term does not apply to phonons at high temperature because the scattering is inelastic and Δ is not negligible. The conductivity due to phonons at high temperatures is solved in ref.[25]

3.3 Magnetic field parallel to the wire axis

3.3.1 Matrix Elements

We make use of the following matrix elements.

$$|\langle nk|\exp(i\vec{q}\cdot\vec{r})|n'k'\rangle|^2 = \frac{n'!}{n!}u^{n'-n}e^{-u}|L_{n'}^{n-n'}(u)|^2 = |J_{nn'}(u)|^2\delta_{k',k-q_x}, \tag{3.52}$$

where the wave function is given in Eq. (2.26) and $u = l^2q_y^2/2$. Also we have the expectation values

$$\langle nk|\alpha_x|nk\rangle = \langle nk|\alpha_y|nk\rangle = 0, \tag{3.53}$$

$$\langle nk|v_x|nk\rangle = \frac{\hbar k_x}{m}, \langle nk|v_y|nk\rangle = 0. \tag{3.54}$$

3.3.2 Conductivity tensor for impurity scattering

Gaussian potential

The matrix elements (3.52)-(3.54) will give a contribution to the conductivity tensor for the diffusion term of σ_{xx}. All other terms are zero including the collision term for σ_{xx} due to the fact that $\langle n, k_x|v_x|n, k_x\rangle$ is the only non-zero matrix element. The relaxation time is given by

$$\frac{1}{\tau} = \frac{N_i V_o^2}{2\pi\hbar A_o}\sum_{n'k_x'}\sum_{q}\exp(-\frac{q_\perp^2 d^2}{2})|J(u)|^2\delta_{k',k-q_x}\delta(\epsilon_\xi - \epsilon_{\xi'}). \tag{3.55}$$

As was done for the case of the magnetic field perpendicular to the wire we assume elastic scattering, convert the sums into integrals, and expand of the $\delta-$function. The relaxation time can then be integrated over q_x to give

$$\frac{1}{\tau} = \frac{mN_iV_o^2L_x}{8\pi^3\hbar^3k_x}\int \exp(-\frac{q_y^2d^2}{2})[\exp(-2k_x^2d^2)+1]|J(\frac{l^2q_y}{2})|^2]dq_y. \tag{3.56}$$

Substituting the relaxation time into Eq.(3.1) gives

$$\sigma_{xx} = \frac{8\pi^3\hbar^5e^2\beta}{m^3N_iV_o^2AL_x}\sum_{n,k_x}\frac{f_{nk_x}(1-f_{nk_x})k_x^3}{\int \exp(-\frac{q_y^2d^2}{2})[\exp(-2k_x^2d^2)+1]|J(\frac{l^2q_y}{2})|^2]dq_y}. \tag{3.57}$$

Using the low temperature limit $f_{n,k_x}(1-f_{n,k_x}) \rightarrow \delta(\epsilon_{n,k_x}-\epsilon_F)$ and converting the sum over k-states into an integral we obtain

$$\sigma_{xx} = \frac{4\pi^2e^2\hbar}{mN_iV_o^2A}\sum_n \frac{E}{I_9(E,q_y)} \tag{3.58}$$

where $E = \epsilon_f - (n+\frac{1}{2})\hbar\varpi$. The function $I_9(E,q_y)$ is an integral over q_y given by

$$I_9(E,q_y) = \left[\exp(-\frac{4d^2Em}{\hbar^2})+1\right]\int dq_y \exp(-a^2q_y^2/2)[|L_n(l^2q_y^2/2)|^2 \tag{3.59}$$

with, $a^2 = d^2+l^2$.

Fig. 3.8 shows Eq. (3.58) plotted as a function of the magnetic field. The function does not have the peak that was present when the magnetic field was perpendicular to the sample, because there is no magnetic field term $1-b^2$. As a result, the dominant term is the numerator $E = \epsilon_f - (n+1/2)\hbar\varpi$ which increases indefinitely with increasing magnetic field. This is to be expected because the

magnetic field parallel to the sample does not produce the oscillatory behavior of the Fermi level that was present in the perpendicular case. The small steps in the conductivity are a result of the integral I_9. As the summation goes through the different Landau levels there is a step down in the value of the integral. This is due to the fact that the number of Landau levels will decrease with increasing field strength, essentially acting to confine the electron.

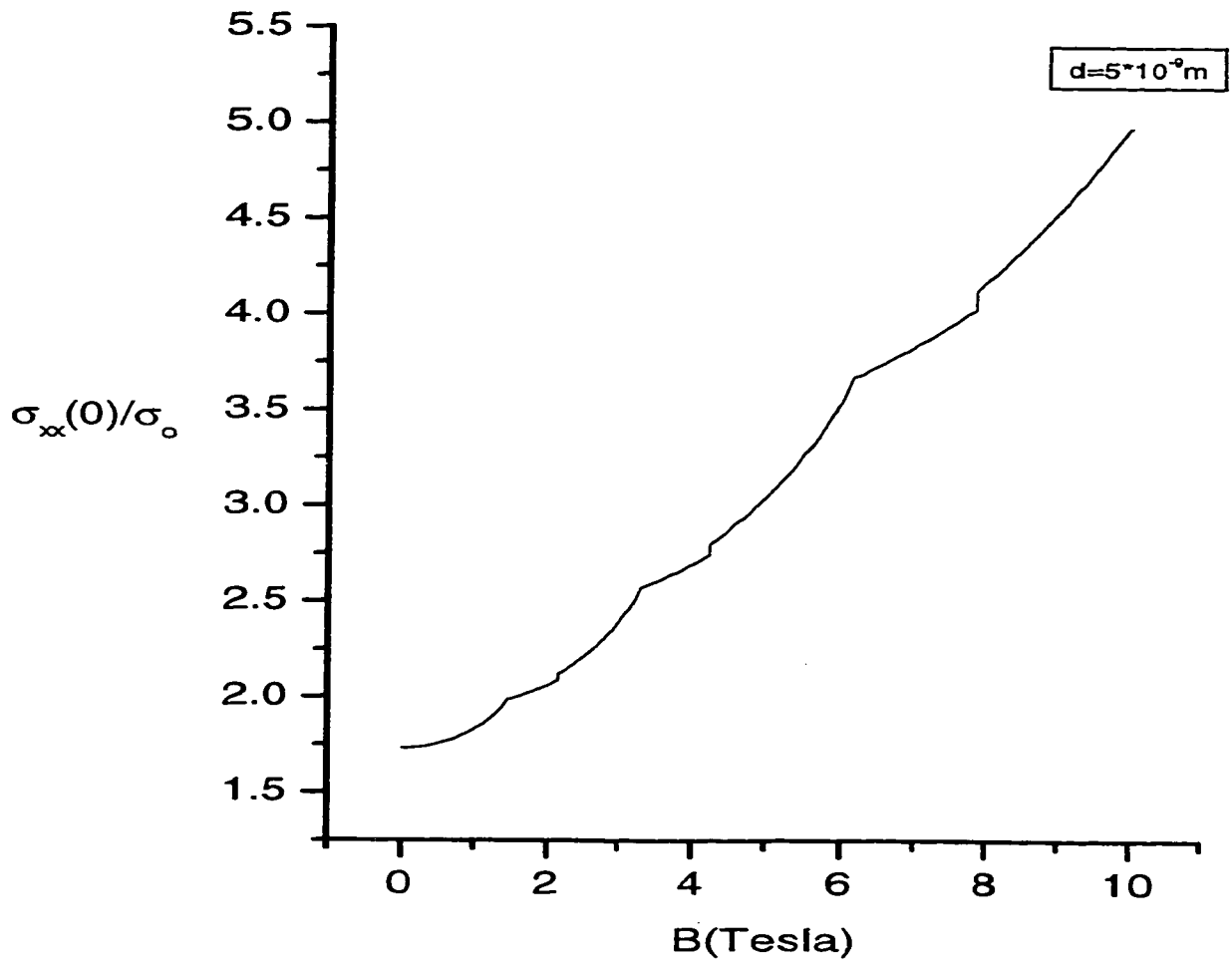

Figure 3.8: Diffusion term of the conductivity as a function of the magnetic field. The scattering potential is Gaussian and $\sigma_o = 10^4 m N_i V_o^2 A / 4\pi^2 e^2 \hbar$.

δ-function potential

As in the case of the Gaussian potential the collision term is zero because the expectation value of the position operator is also zero. The diffusion term is given by Eq. (3.1) and the relaxation time can be found by using the elastic scattering approximation ($n' \rightarrow n$) and converting the sums into integrals to give

$$\frac{1}{\tau} = \frac{N_i V^2 m L_x}{8\pi^3 \hbar^3 k_x} \int dq_y |J_n(\frac{l^2 q_y^2}{2})|^2. \tag{3.60}$$

Substituting Eq. (3.60) into Eq. (3.1) and using the low- temperature limit gives

$$\sigma_{xx} = \frac{8\pi^2 e^2 \hbar}{A N_i V^2 m} \sum_n \frac{E}{\int dq_y |J_n(\frac{l^2 q_y^2}{2})|^2}. \tag{3.61}$$

Fig. 3.9 shows Eq. (3.60) plotted as a function of the magnetic field. The graph is simply the same result as the Gaussian potential and the reasoning is also the same.

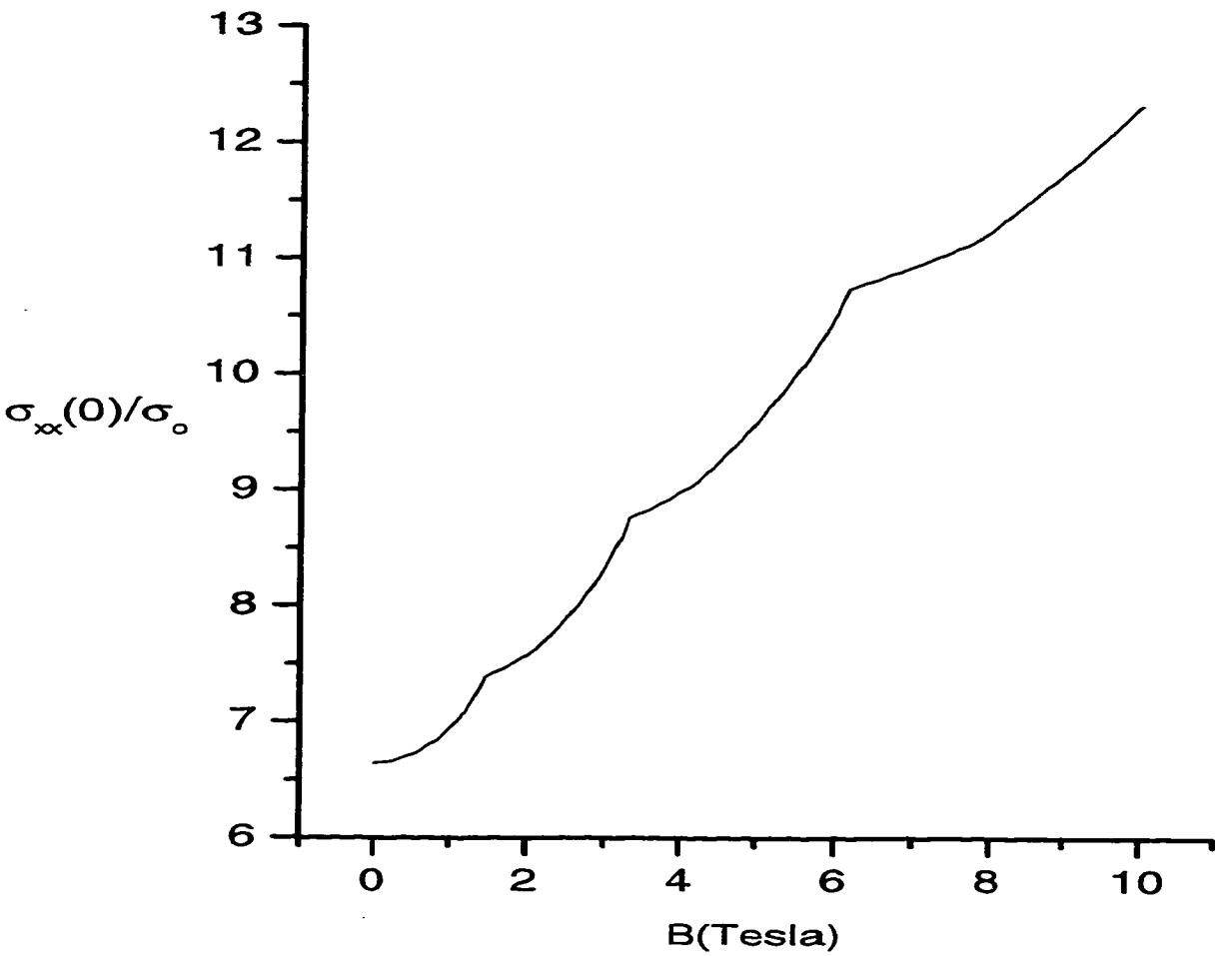

Figure 3.9: Diffusion term of the conductivity as a function of the magnetic field. The scattering potential is a $\delta-$function, and $\sigma_o = 10^7 m N_i V_o^2 A/8\pi^3\hbar$.

Screened Coulomb potential

The conductivity tensor for the screened Coulomb potential is found by inserting Eq. (3.7) into Eq. (3.4). Following the same procedure as in the previous two elastic potentials we have

$$\sigma_{xx} = \frac{\hbar\epsilon}{2\pi m A N_i} \sum_n \frac{E}{\int dq_y |J_n(\frac{l^2 q_y^2}{2})|^2 [\frac{4mE}{\hbar^2} + q_y^2 + k_s^2]}. \tag{3.62}$$

3.3.3 Conductivity tensors for phonon scattering

Similar to the impurity scattering the collision term of the conductivity tensor will be zero because the matrix elements are all zero. The diffusion term of the conductivity tensor can be found in the same way that the it was found for the case where the magnetic field is perpendicular to the wire. Expanding the δ function in Taylor series and eliminating odd terms as well as higher-order terms the diffusion term cam be written as

$$\sigma_{xx} = \frac{2\beta e^2 \hbar^4 \varpi}{A_o L_x m^2} \frac{1}{[1 + 2\sum_s (-1)^s \cos(2\pi s \Delta)]}$$

$$\times \sum_{n,k_x} \frac{f_{n,k_x}(1 - f_{n,k_x}) k_x^2}{\sum_q |F(q)|^2 [N_o |J_{n\pm\Delta}(u)|^2]} \tag{3.63}$$

Acoustic phonons at low temperatures

Substituting the Eq. (3.13) for acoustic phonons and converting the Fermi functions into a δ function in the low-temperature limit, the conductivity tensor is

$$\sigma_{xx} = \frac{2e^2\hbar\varpi}{\alpha\sqrt{2m}} \sum_{n,k_x} \frac{1}{1+2\sum_s (-1)^s \cos(2\pi s\Delta)} \frac{\sqrt{E}}{\sum_q q_\perp N_o |J_{n\pm\Delta}(u)|^2} \tag{3.64}$$

3.4 Conclusion

The dc conductivity tensor was found for various interactions of the electrons with scattering potentials. The confining potential was always strictly harmonic, this was done to see what the dominant terms in the conductivities might be and whether a different confining potential would actually result in any appreciable difference in the conductivities.

When the magnetic field is perpendicular to the wire, the dominant term is due to the magnetic field through the expectation operators for position and velocity. As a result, the rather small effect the confining potential has on the conductivity through the Fermi level is not large enough to notice. Also, because we have previously established that the Fermi level does not change much due to the presence of anharmonic terms in the confining potential, we can assert that there would be minimal contribution from these terms to the conductivity. This may prove to be different if the corrected wave function were to be used to determine the

expectation values but then the problem would no longer be tractable.

On the other hand, if the magnetic field is parallel to the motion of the electron the dominant term is no longer due to the expectation values. The dominant term would be the summation over n states in the conductivity. The two main contributions to these summations seem to be coming from the Fermi level and the scattering potential. The Fermi level we know will not change much with the addition of small-order terms to the confining potential. The scattering potential does not have any common parameters with the confining potential, so it is difficult to see how anharmonic terms would change anything. In fact, the physical parameters of the scattering potentials, i.e., k_s, the inverse screening length and d the range of the Gaussian potential seem to have a much larger affect on the result of conductivity than anything else.

Chapter 4

Power Spectrum

Within this chapter we look at the response of the quantum wire when an a.c. current is applied across it. In order to determine what the response will be we study the power spectrum of the wire, that is the power absorbed by the quantum wire given an electric field, E ,is applied in the direction of the electron motion (in this case the x direction). The formula for the power spectrum, for circularly polarized light of frequency ω and electric-field strength E, is given by [21]

$$P(\omega) = \frac{1}{2}E^2\sigma_{\pm}. \tag{4.1}$$

In this equation $\sigma_{\pm}$ is the dynamic conductivity tensors given by

$$\sigma_{\pm} = Re[\sigma_{xx}(\omega) + \sigma_{yy}(\omega) - i\sigma_{xy}\omega + i\sigma_{yx}(\omega)]. \tag{4.2}$$

When determining the power spectrum experimentally, the constraint $\omega_c\tau \gg 1$ is placed upon the system and leads to the result $\sigma_{\mu\nu}^{(nd)}(\omega) \gg \sigma_{\mu\nu}^{(d)}(\omega)$, see [21]. The nondiagonal conductivity tensors are given in Ref.[21] by

$$\sigma_{\mu\nu}(\omega) = \frac{i\hbar e}{\omega} \sum_{\xi' \neq \xi} \frac{f_\xi - f_{\xi'}}{E_\xi - E_{\xi'}} \langle \xi | v_\mu | \xi' \rangle \langle \xi' | v_\nu | \xi \rangle \lim_{\epsilon \to 0} \frac{1}{E_\xi - E_{\xi'} + \hbar\omega + i\epsilon}, \tag{4.3}$$

where f_ξ is the Fermi-dirac distribution, $\langle \xi | v_\mu | \xi' \rangle$ the velocity matrix element, and E_ξ is the one electron eigenvalues found in Chapter 1.

4.1 Magnetic field perpendicular to the wire

4.1.1 Velocity matrix elements

The off-diagonal elements are not normally present but the multiplication of the velocity matrices leads to real effects in Eq. (4.3). The wave functions are those found for a magnetic field perpendicular to a quantum wire with a confinement potential $\Omega y^2 + \delta V(y)$, where $\delta V(y)$ is the perturbation. The perturbation is small enough relative to the unpertubed term that the corrections to the eigenfunctions can be ignored when determinng the velocity matrices. By evaluation of the formula $\langle n, k_x | v_\mu | n' k_x' \rangle$ we obtain

$$\langle nk_x|v_x|n'k'_x\rangle = \left[\frac{\hbar k_x}{m}(1-\frac{\omega_c^2}{\varpi^2})\right]\delta_{nn'}\delta_{k_xk'_x}$$

$$+\frac{\omega_c}{\alpha}\left[\sqrt{\frac{n'}{2}}\delta_{nn'-1}+\sqrt{\frac{n'+1}{2}}\delta_{nn'+1}\right]\delta_{k_xk'_x}, \qquad (4.4)$$

$$\langle nk_x|v_y|n'k'_x\rangle = \frac{i\hbar\alpha}{m}\left[-\sqrt{\frac{n'}{2}}\delta_{nn'-1}+\sqrt{\frac{n'+1}{2}}\delta_{nn'+1}\right]\delta_{k_xk'_x}. \qquad (4.5)$$

4.1.2 Conductivity tensor

The nondiagonal element tensor is given by Eq.(4.3). Inserting the velocity matrix elements Eq. (4.4)and (4.5)into (4.3) gives

$$\sigma_{xx}^{nd}(\omega) = \frac{i\hbar e^2}{2mA_o}\left(\frac{\hbar\omega_c^2}{\varpi}\right)\sum_{nk_x}[\frac{f_{n,k_x}-f_{n+1,k_x}}{\varepsilon_{n,k_x}-\varepsilon_{n+1,k_x}}\lim_{\varepsilon\to 0}\frac{(n+1)}{\varepsilon_{n,k_x}-\varepsilon_{n+1,k_x}+\hbar\omega+i\varepsilon}$$

$$+\frac{f_{n,k_x}-f_{n-1,k_x}}{\varepsilon_{n,k_x}-\varepsilon_{n-1,k_x}}\lim_{\varepsilon\to 0}\frac{n}{\varepsilon_{n,k_x}-\varepsilon_{n-1,k_x}+\hbar\omega+i\varepsilon}]. \qquad (4.6)$$

If we let $n \to n+1$ in the second term of the the sum and rearrange terms we obtain,

$$\sigma_{xx}^{nd}(\omega) = \frac{i\hbar e^2}{2mA_o}\left(\frac{\hbar\omega_c^2}{\varpi}\right)\sum_{nk_x}[\frac{f_{n,k_x}-f_{n+1,k_x}}{\Delta_{n+1,k_x}}(n+1)\lim_{\varepsilon\to 0}\frac{1}{\Delta_{n+1,k_x}-\hbar\omega-i\varepsilon}$$

$$+\frac{f_{n,k_x}-f_{n+1,k_x}}{\Delta_{n+1,k_x}}(n+1)\lim_{\varepsilon\to 0}\frac{-1}{\Delta_{n+1,k_x}+\hbar\omega+i\varepsilon}] \tag{4.7}$$

where $\Delta_{n+1,k_x} = \varepsilon_{n+1,k_x} - \varepsilon_{n,k_x}$. Assuming broadening of the energy levels due to collisions, we can make the change $\varepsilon \to \Gamma$, where Γ is the level width. Simplifying further by multiplying both the numerator and denominator in the sums by their complex conjugate, we obtain for the conductivity

$$\sigma_{xx}^{nd}(\omega) = \frac{i\hbar e^2}{2mA_o}\left(\frac{\hbar\omega_c^2}{\varpi}\right)\sum_{nk_x}\frac{f_{n,k_x}-f_{n+1,k_x}}{\Delta_{n+1,k_x}}(n+1)$$

$$\times\left[\frac{\Delta_{n+1,k_x}-\hbar\omega+i\Gamma}{(\Delta_{n+1,k_x}-\hbar\omega)^2+\Gamma^2}+\frac{-(\Delta_{n+1,k_x}+\hbar\omega)+i\Gamma}{(\Delta_{n+1,k_x}+\hbar\omega)^2+\Gamma^2}\right]. \tag{4.8}$$

This expression is valid for any confining potential, with Δ_{n+1,k_x} being the difference between consecutive energy levels.

The remaining components of the conductivity tensor are found following the same steps as above. For $\sigma_{yy}^{nd}(\omega)$ we obtain

$$\sigma_{yy}^{nd} = \frac{i\hbar^2 e^2\varpi}{2mA_o}\sum_{nk_x}\frac{f_{n,k_x}-f_{n+1,k_x}}{\varepsilon_{n,k_x}-\varepsilon_{n+1,k_x}}(n+1)\lim_{\varepsilon\to 0}\frac{1}{\varepsilon_{n,k_x}-\varepsilon_{n+1,k_x}+\hbar\omega+i\varepsilon}$$

$$+\frac{f_{n,k_x}-f_{n-1,k_x}}{\varepsilon_{n,k_x}-\varepsilon_{n-1,k_x}}(n)\lim_{\varepsilon\to 0}\frac{1}{\varepsilon_{n,k_x}-\varepsilon_{n-1,k_x}+\hbar\omega+i\varepsilon}. \tag{4.9}$$

Again performing the same substitution into the second term and rearranging the energy and Fermi functions, with $\varepsilon \to \Gamma$, gives

$$\sigma_{yy}^{nd} = \frac{i\hbar^2 e^2 \varpi}{2mA_o} \sum_{nk_x} \frac{f_{n,k_x} - f_{n+1,k_x}}{\Delta_{n+1,k_x}} (n+1)$$

$$\times \left[\frac{\Delta_{n+1,k_x} - \hbar\omega + i\Gamma}{(\Delta_{n+1,k_x} - \hbar\omega)^2 + \Gamma^2} - \frac{(\Delta_{n+1,k_x} + \hbar\omega) - i\Gamma}{(\Delta_{n+1,k_x} + \hbar\omega)^2 + \Gamma^2} \right]. \quad (4.10)$$

For the last two conductivity components the relation $\sigma_{yx}^{nd} = -\sigma_{xy}^{nd}$ holds, so that only one of the two need be calculated. Multiplying the velocity matrix elements and summing over the ξ' states leads to

$$\sigma_{yx}^{nd}(\omega) = \frac{\hbar^2 e^2 \omega_c}{2mA_o} \sum_{nk_x} \frac{f_{n,k_x} - f_{n+1,k_x}}{\Delta_{n+1,k_x}} (n+1)$$

$$\times \left[\frac{\Delta_{n+1,k_x} - \hbar\omega + i\Gamma}{(\Delta_{n+1,k_x} - \hbar\omega)^2 + \Gamma^2} + \frac{\Delta_{n+1,k_x} + \hbar\omega - i\Gamma}{(\Delta_{n+1,k_x} + \hbar\omega)^2 + \Gamma^2} \right]. \quad (4.11)$$

4.1.3 Power spectrum

The above components of the conductivity tensor are inserted in Eq. (4.1) and the power spectrum is found to be

$$P(\omega) = \frac{\hbar^2 e^2 E^2}{4m\varpi A_o} \sum_{n,k_x} \frac{f_{n+1,k_x} - f_{n,k_x}}{\Delta_{n+1,k_x}} (n+1)\,\Gamma$$

$$\times \left[\frac{(\omega_c + \varpi)^2}{(\Delta_{n+1,k_x} - \hbar\omega)^2 + \Gamma^2} + \frac{(\omega_c - \varpi)^2}{(\Delta_{n+1,k_x} + \hbar\omega)^2 + \Gamma^2} \right]. \quad (4.12)$$

$\Gamma =$ **constant**

The above result Eq. (4.12) can be simplified for some special forms of Γ,e.g. when Γ is a constant, or when there is short-range scattering due to impurities, such as δ-function scattering. If Γ is a constant, then the summation over k_x states can be converted into an integral $\sum \rightarrow L_x \int dk_x/2\pi$ and $P(\omega)$ can be put into the form

$$P(\omega) = \frac{\hbar^2 e^2 E^2 \Gamma}{8\pi m \varpi L_y} \sum_n \int dk_x \frac{f_{n+1,k_x} - f_{n,k_x}}{\Delta_{n+1,k_x}} (n+1)$$

$$\times \left[\frac{(\omega_c + \varpi)^2}{(\Delta_{n+1,k_x} - \hbar\omega)^2 + \Gamma^2} + \frac{(\omega_c - \varpi)^2}{(\Delta_{n+1,k_x} + \hbar\omega)^2 + \Gamma^2} \right]. \quad (4.13)$$

When the confining potential is harmonic($\Delta_{n+1,k_x} = \hbar\varpi$) this expression can be further simplified to give

$$P(\omega) = \frac{\hbar e^2 E^2 \Gamma}{8\pi m \varpi^2 L_y} \left[\frac{(\omega_c + \varpi)^2}{(\hbar\varpi - \hbar\omega)^2 + \Gamma^2} + \frac{(\omega_c - \varpi)^2}{(\hbar\varpi + \hbar\omega)^2 + \Gamma^2} \right]$$

$$\times \sum_n \int dk_x (n+1) (f_{n+1,k_x} - f_{n,k_x}) \quad (4.14)$$

Figure 4.1 shows the power spectrum for three different confining potentials as a function of the magnetic field with a constant value for Γ. The strength of the confining potential has very little effect upon the power spectrum, with the curves being almost identical, i.e., there is less than a 1% difference between the three

graphs, with a 20% difference between corrected and uncorrected eigenvalues.

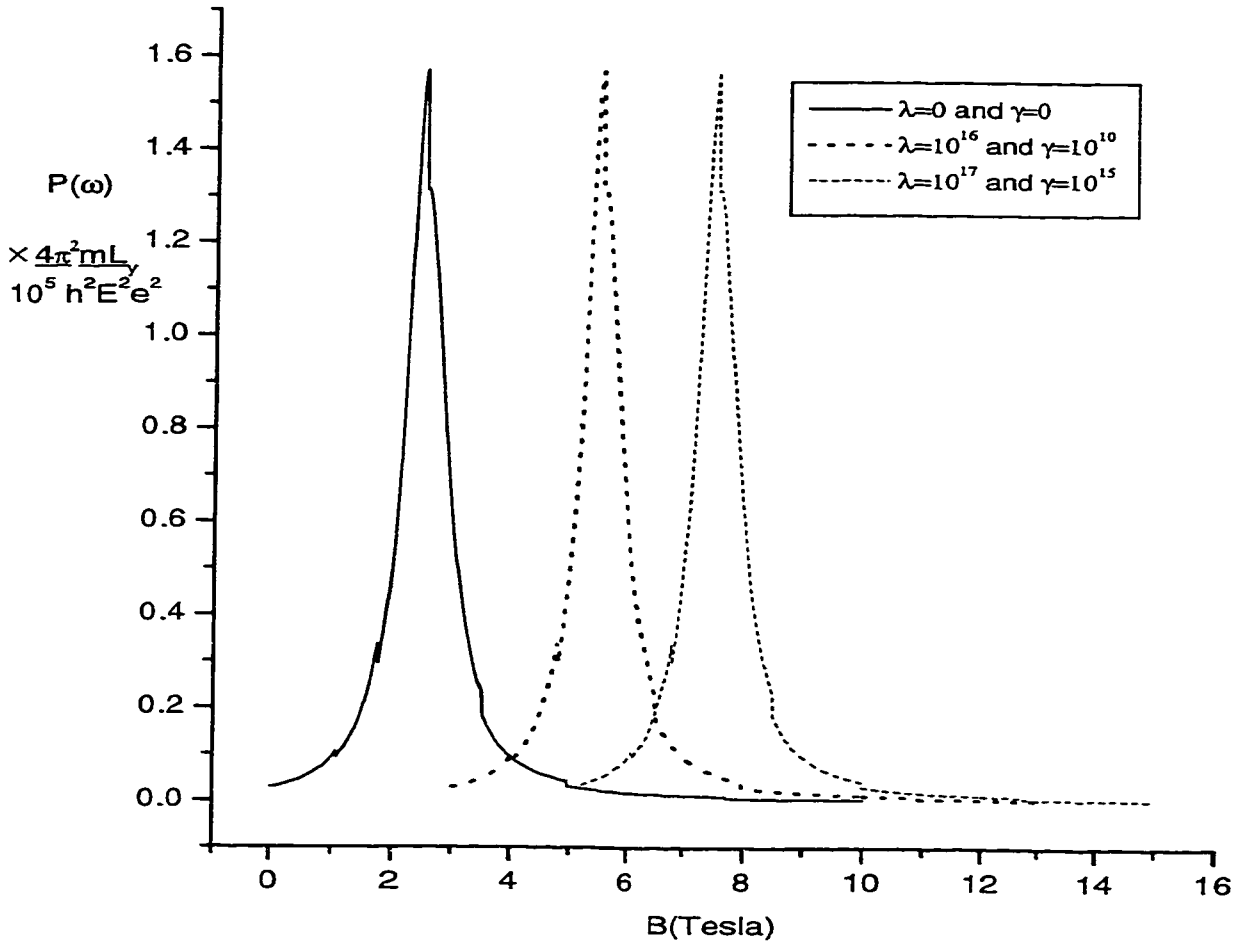

Figure 4.1: Power spectrum for three different confining potentials. The curves for the corrected potentials have been shifted along the x axis. $\Gamma = .5$meV, λ has units of eV/m^3 and γ has units of eV/m^4.

$\Gamma \neq constant$

When Γ is not a constant but depends on the magnetic field and/or k_x, an expression for it can be found for short-range scattering (see [20], p.537)

$$\Gamma^2 = \frac{2}{\pi}\frac{\hbar^2\omega_c}{\tau_F} = \frac{2\hbar^2\omega_c}{\pi}\sum_{\xi'} W_{\xi\xi'}(B=0), \tag{4.15}$$

with $W_{\xi\xi'}$ being the transition matrix element given by Fermi's Golden rule [9].

The integral, $\langle n, k_x|\exp(\imath\vec{q}\cdot\vec{r})|n', k_x'\rangle$ can be evaluated using [12], if the wave functions are obtained from an harmonic confining potential,

$$\langle n, k_x|\exp(\imath\vec{q}\cdot\vec{r})|n', k_x'\rangle = |J_{nn'}(u)|^2\delta_{k_x,k_x-q_x}, \tag{4.16}$$

where $|J_{nn'}(u)|^2 = u^{\frac{1}{2}}\exp(-u)\,|L_n^{n'-n}(u)|^2$ and $L_n^{n'-n}(u)$ is a Laguerre polynomial. Using Eq. (4.15) and (4.16), we obtain

$$\Gamma^2 = \frac{4\hbar\omega_c}{A_o}\sum_{n',k_x'}\sum_{q}|U(q)|^2|J_{nn'}(u)|^2\delta_{k_x,k_x-q_x}\delta\left(\epsilon_n(k_x)-\epsilon_{n'}(k_x')\right). \tag{4.17}$$

where $|U(q)|^2$ is the Fourier transform of the scattering potential. This expression can be simplified when simple scattering mechanisms are considered. Since the above equation is valid for short-range scattering only, then we use the result $|U(q)|^2 = V_o^2$ valid for δ-function scattering or the Guassian potential $|U(q)|^2 = V_o^2\exp(-q_\perp^2 d^2/2)/4\pi^2$, which behaves like the δ-function potential in the limit $d \to 0$. We may further simplify, Eq. (4.17), if the sums over k_x' and q are

converted to integrals and the confining potential is harmonic. For δ-function scattering this gives

$$\Gamma^2 = \frac{mV_o^2\omega_c L_x}{2\pi^3\hbar k_x}\int dq_x dq_y |J_n\left(\frac{l^2q_\perp^2}{2}\right)|^2\left[\delta\left(q_x-2k_x\right)+\delta\left(q_x\right)\right]. \tag{4.18}$$

Integrating this expression with respect to q_x gives

$$\Gamma^2 = \frac{mV_o^2\omega_c L_x}{8\pi^5\hbar k_x}\int dq_y \left[|J_n\left(l^2A_{xy}\right)|^2+|J_n\left(\frac{l^2q_y^2}{2}\right)|^2\right], \tag{4.19}$$

where $A_{xy} = \left(4k_x^2+q_y^2\right)/2$.

If the scattering potential is Gaussian then, we can follow the same steps as we did to arrive at Eq.(4.19). The result is

$$\Gamma^2 = \frac{mV_o^2\omega_c L_x}{2\pi^3\hbar k_x}\int dq_y$$

$$\times\left[\exp\left(-d^2A_{xy}\right)\left|J_n\left(l^2A_{xy}\right)\right|^2+\exp\left(\frac{-q_y^2d^2}{2}\right)\left|J_n\left(\frac{l^2q_y^2}{2}\right)\right|^2\right] \tag{4.20}$$

The result given for the power spectrum in Eq. (4.12) can be put into the form

$$P(\omega) = \frac{\hbar^2e^2E^2}{8\pi m\varpi L_y}\sum_n\int dk_x\left[\frac{f_{n+1,k_x}-f_{n,k_x}}{\Delta_{n+1,k_x}}\right](n+1)\,\Gamma\left(k_x\right)$$

$$\times\left[\frac{\left(\omega_c+\varpi\right)^2}{\left(\Delta_{n+1,k_x}-\hbar\omega\right)^2+\Gamma\left(k_x\right)^2}+\frac{\left(\omega_c-\varpi\right)^2}{\left(\Delta_{n+1,k_x}+\hbar\omega\right)^2+\Gamma\left(k_x\right)^2}\right] \tag{4.21}$$

with the integral over q_y having to be solved numerically when $\Gamma\left(k_x\right)$ is replaced by either eq.(4.19), or eq.(4.20).

4.2 Magnetic field in the plane and perpendicular to the electron motion

4.2.1 Velocity matrix elements

The results velocity matrix elements are found using the wave function of Eq.(2.40). They are

$$\langle nsk_x|v_x|n's'k'_x\rangle = \left[\frac{\hbar k_x}{m}(1-\frac{\omega_c^2}{\varpi^2})\right]\delta_{ss'}\delta_{nn'}\delta_{k_x,k'_x} + \omega_c l\left[\sqrt{\frac{s'}{2}}\delta_{ss'-1}+\sqrt{\frac{s'+1}{2}}\delta_{ss'+1}\right]\delta_{nn'}\delta_{k_x,k'_x}, \quad (4.22)$$

$$\langle nsk_x|v_y|n's'k'_x\rangle = \frac{-i\hbar}{l_n m}\left[\sqrt{\frac{n'}{2}}\delta_{nn'-1}-\sqrt{\frac{n'+1}{2}}\delta_{nn'+1}\right]\delta_{ss'}\delta_{k_x,k'_x}, \quad (4.23)$$

$$\langle nsk_x|v_z|n's'k'_x\rangle = \frac{-i\hbar}{lm}\left[\sqrt{\frac{s'}{2}}\delta_{ss'-1}-\sqrt{\frac{s'+1}{2}}\delta_{ss'+1}\right]\delta_{nn'}\delta_{k_x,k'_x}. \quad (4.24)$$

4.2.2 Conductivity Tensors

We insert these matrix elements in Eq. (4.1) as well as the eigenvalues of Eq.(2.41). We further assume that the only occupied subband among the s-states

is the s=0 subband. We can make this assumption because the confinement in the z-direction is much higher than the confinement in all other directions. In all other respects, the derivation of the conductivity tensors is identical to the procedure that was followed to determine $\sigma_{\pm}$ when the magnetic field is perpendicular to the plane of the quantum wire. The conductivity nondiagonal components are found to be

$$\sigma_{xx}^{nd}(\omega) = \frac{i(\omega_c l_s)^2 e^2}{V_o m \varpi} \sum_{nk_x} (f_{n,k_x,1} - f_{n,k_x,0}) \times \left[\frac{\hbar\varpi + \hbar\omega - i\Gamma}{(\hbar\varpi + \hbar\omega)^2 + \Gamma^2} - \frac{\hbar\varpi - \hbar\omega + i\Gamma}{(\hbar\varpi - \hbar\omega)^2 + \Gamma^2} \right], \tag{4.25}$$

$$\sigma_{yy}(\omega) = \frac{i\hbar e^2}{V_o (l_n m)^2 \Omega} \sum_{nk_x} (f_{n+1,k_x,0} - f_{n,k_x,0}) \left(\frac{n+1}{2} \right) \times \left[\frac{\hbar\Omega + \hbar\omega - i\Gamma}{(\hbar\Omega + \hbar\omega)^2 + \Gamma^2} - \frac{\hbar\Omega - \hbar\omega + i\Gamma}{(\hbar\Omega - \hbar\omega)^2 + \Gamma^2} \right], \tag{4.26}$$

and

$$\sigma_{zz}(\omega) = \frac{i\hbar e^2}{2V_o (l_s m)^2 \varpi} \sum_{nk_x} (f_{n+1,k_x,0} - f_{n,k_x,0}) \times \left[\frac{\hbar\Omega + \hbar\omega - i\Gamma}{(\hbar\Omega + \hbar\omega)^2 + \Gamma^2} - \frac{\hbar\Omega - \hbar\omega + i\Gamma}{(\hbar\Omega - \hbar\omega)^2 + \Gamma^2}](\hbar\Omega - \hbar\omega)^2 + \Gamma^2 \right] \tag{4.27}$$

The cross terms in the tensors are given by

$$\sigma_{zx}(\omega) = -\sigma_{xz}(\omega), \tag{4.28}$$

$$\sigma_{xy} = \sigma_{zx} = \sigma_{yz} = \sigma_{zy} = 0, \tag{4.29}$$

with

$$\sigma_{xz}(\omega) = \frac{\hbar e^2 \omega_c}{2V_o m\varpi} \sum_{nk_x} (f_{n,k_x,1} - f_{n,k_x,0})$$

$$\times \left[\frac{\hbar\Omega + \hbar\omega - i\Gamma}{(\hbar\Omega + \hbar\omega)^2 + \Gamma^2} - \frac{\hbar\Omega - \hbar\omega + i\Gamma}{(\hbar\Omega - \hbar\omega)^2 + \Gamma^2} \right]. \tag{4.30}$$

4.2.3 Power spectrum

Inserting the conductivity components (4.25)-(4.30) in Eq. (4.1) and converting the sum over k_x into an integral gives

$$P(\omega) = \frac{\hbar e^2 E^2 L_x \Gamma}{8\pi m V_o}$$

$$\times \sum_n \int dk_x \left[f_{n+1,k_x,0} - f_{n,k_x,0} \right] (n+1) \left[\frac{1}{(\hbar\Omega + \hbar\omega)^2 + \Gamma^2} + \frac{1}{(\hbar\Omega - \hbar\omega)^2 + \Gamma^2} \right]$$

$$+ \left[f_{n,k_x,1} - f_{n,k_x,0} \right] \left[\frac{(\frac{\omega_c}{\varpi} - 1)^2}{(\hbar\varpi + \hbar\omega)^2 + \Gamma^2} - \frac{(\frac{\omega_c}{\varpi} + 1)^2}{(\hbar\varpi - \hbar\omega)^2 + \Gamma^2} \right]. \tag{4.31}$$

4.3 Magnetic field in the (x-z) plane

4.3.1 Velocity matrix elements

Using the wave function of Eq.(2.46) velocity matrix elements are

$$\langle nk_x|v_x|n'k'_x\rangle = \left[\frac{\hbar k_x}{m}(1-\frac{\omega_\perp^2}{\varpi^2})\right]\delta_{nn'}\delta_{k_x,k'_x}$$

$$+\omega_\perp\tilde{l}\left[\sqrt{\frac{n'}{2}}\delta_{nn'-1}+\sqrt{\frac{n'+1}{2}}\delta_{nn'+1}\right]\delta_{k_x,k'_x}, \qquad (4.32)$$

$$\langle nk_x|v_y|n'k'_x\rangle = \frac{-i\hbar}{\tilde{l}m}\left[-\sqrt{\frac{n'}{2}}\delta_{nn'-1}+\sqrt{\frac{n'+1}{2}}\delta_{nn'+1}\right]\delta_{k_x,k'_x}. \qquad (4.33)$$

4.3.2 Conductivity tensor

Following, the same procedures as in prevous orientations of the magnetic field, with the eigenvalues of Eq. (2.47), the conductivity components are

$$\sigma_{xx}(\omega) = \frac{i\omega_\perp^2\hbar e^2}{A_o m\varpi^2}\sum_{nk_x}(f_{n,k_x}-f_{n,k_x})(n+1)$$

$$\times\left[\frac{\hbar\varpi+\hbar\omega-i\Gamma}{(\hbar\varpi+\hbar\omega)^2+\Gamma^2}-\frac{\hbar\varpi-\hbar\omega+i\Gamma}{(\hbar\varpi-\hbar\omega)^2+\Gamma^2}\right], \qquad (4.34)$$

and

$$\sigma_{yy} = \frac{\varpi^2}{\omega_\perp}\sigma_{xx}, \tag{4.35}$$

$$\sigma_{xy} = -\sigma_{yx} = \frac{\varpi}{\omega_\perp}\sigma_{xx}. \tag{4.36}$$

4.3.3 Power spectrum

The conductivity components (4.34)-(4.36) can be inserted into Eq.(4.1) and the sum over k_x states converted to an integral to give

$$P(\omega) = \frac{\hbar e^2 E^2 \Gamma}{4\pi m L_y \varpi^2} \sum_n \int dk_x [f_{n+1,k_x} - f_{n,k_x}](n+1)$$

$$\times \left[\frac{(\omega_\perp - \varpi)^2}{(\hbar\varpi + \hbar\omega)^2 + \Gamma^2} + \frac{(\omega_\perp + \varpi)^2}{(\hbar\varpi - \hbar\omega)^2 + \Gamma^2} \right]. \tag{4.37}$$

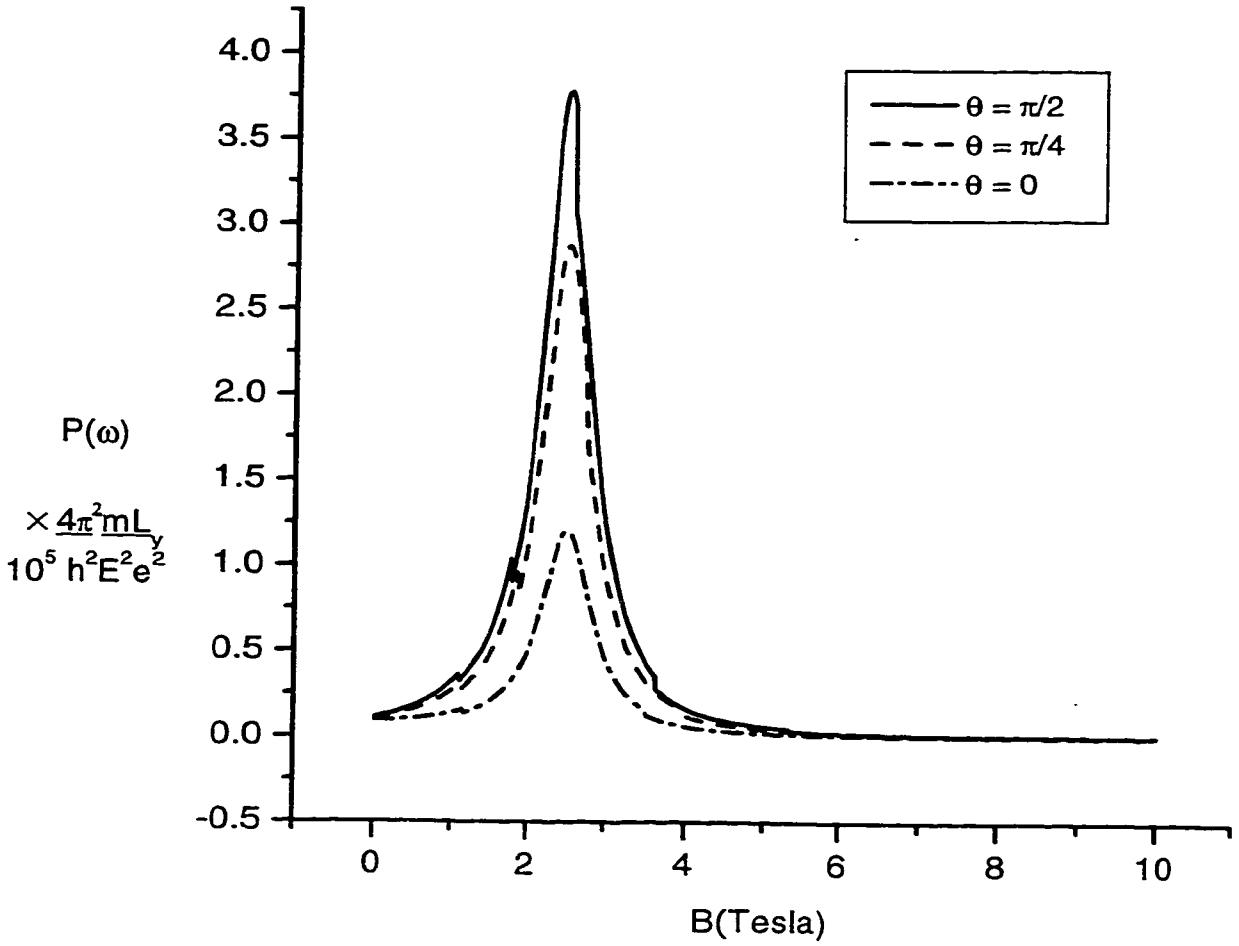

Figure 4.2: Power spectrum for three different orientations of the magnetic field , the power spectrum peak drops as the angle of the B-field is lowered. The width is $\Gamma = .5$meV and the magnetic field strength is given by $B = \sqrt{B_x^2 + B_z^2}$.

Figure 4.2 shows the power spectrum given different orientations of the magnetic field in the (x-z) plane. As expected, the power spectrum response weakens as the magnetic field is tilted towards the x axis of the quantum wire parallel to the electron motion. From the graph and Eq. 4.37 it is obvious that adding an anharmonic term to the confinement potential will once again not affect the power spectrum response of the wire.

4.4 Magnetic field in the (x-y) plane of a wire with finite thickness

4.4.1 velocity matrix elements

The velocity matrix elements are found using the wave function of Eq.(2.50) and the velocity operator

$$[v_x, v_y, v_z] = -\frac{1}{m}\left[\imath\hbar\frac{\partial}{\partial x} - eB_{\models}z, \imath\hbar\frac{\partial}{\partial y} + eB_{\|}z, \imath\hbar\frac{\partial}{\partial z}\right]. \tag{4.38}$$

The results are

$$\begin{aligned}\langle nk_x|v_x|n'k'_x\rangle \quad &= \left[\frac{\hbar k_x}{m}(1-\frac{\omega_{\models}^2}{\varpi^2})\right]\delta_{nn'}\delta_{mm'}\delta_{k_x,k'_x} \\ &+\omega_{\models}\tilde{l}_n\left[\sqrt{\frac{n'}{2}}\delta_{nn'-1} + \sqrt{\frac{n'+1}{2}}\delta_{nn'+1}\right]\delta_{mm'}\delta_{k_x,k'_x}, \end{aligned}\tag{4.39}$$

$$\langle nk_x|v_y|n'k_x'\rangle = \frac{\imath\hbar}{\tilde{l}_m}\left[-\sqrt{\frac{m'}{2}}\delta_{mm'-1} + \sqrt{\frac{m'+1}{2}}\delta_{mm'+1}\right]\delta_{nn'}\delta_{k_x,k_x'} +$$

$$\omega_{||}\tilde{l}_n\left[\sqrt{\frac{n'}{2}}\delta_{nn'-1} + \sqrt{\frac{n'+1}{2}}\delta_{nn'+1}\right]\delta_{mm'}\delta_{k_x,k_x'}, \tag{4.40}$$

and

$$\langle nk_x|v_z|n'k_x'\rangle = \frac{\imath\hbar}{m\tilde{l}_n}\left[-\sqrt{\frac{n'}{2}}\delta_{nn'-1} + \sqrt{\frac{n'+1}{2}}\delta_{nn'+1}\right]\delta_{mm'}\delta_{k_x,k_x'}. \tag{4.41}$$

4.4.2 Conductivity tensor

Inorder to simplify the calculation of the conductivity we again consider only the $n = 0$ subband because of the strong confinement in the z-direction. The result for $\sigma_{xx}^{(}nd)(\omega)$

$$\sigma_{xx}^{nd}(\omega) = \frac{i\hbar^2\omega_{\models}^2 e^2}{2A_o\tilde{m}\varpi}\sum_{mk_x}\frac{(f_{m,1k_x} - f_{m,0,k_x})}{\hbar\varpi + \Delta}$$

$$\times\left[\frac{\hbar\varpi + \hbar\omega - i\Gamma}{F_+} - \frac{\hbar\varpi - \hbar\omega + i\Gamma}{F_-}\right] \tag{4.42}$$

where, $\Delta = (m + 1/2)\hbar\omega_{||}^3\Omega^2/\varpi^2(\varpi^2 - \omega_{||}^2)$, $F_+ = (\hbar\varpi + \Delta + \hbar\omega)^2 + \Gamma^2$, and $F_- = (\hbar\varpi + \Delta - \hbar\omega)^2 + \Gamma^2$. The other conductivity components are found in a similar manner. We obtain

$$\sigma_{xy} = \sigma_{yx} = -\frac{\omega_{||}}{\omega_{\models}}\sigma_{xx}, \tag{4.43}$$

$$\sigma_{xz} = -\sigma_{zx} = \frac{\hbar^2 \omega_{\models} e^2}{2A_o \tilde{m}} \sum_{mk_x} (f_{m,1,k_x} - f_{m,0,k_x})$$

$$\times \left[\frac{\hbar\varpi + \hbar\omega - i\Gamma}{F_+} + \frac{\hbar\varpi - \hbar\omega + i\Gamma}{F_-} \right], \tag{4.44}$$

$$\sigma_{yy} = \frac{\omega_{\|}^2}{\omega_{\models}^2} \sigma_{xx} + \frac{\imath\hbar e^2 \Omega}{2A_o \tilde{m}} \sum_{mk_x} (f_{m+1,0,k_x} - f_{m,0,k_x})(m+1)$$

$$\times \left[\frac{\hbar\varpi + \hbar\omega - i\Gamma}{\Delta_{m_+}^2 + \Gamma^2} - \frac{\hbar\varpi - \hbar\omega + i\Gamma}{\Delta_{m_-}^2 + \Gamma^2} \right], \tag{4.45}$$

$$\sigma_{zz} = \frac{\varpi^2}{\omega_{\models}^2} \sigma_{xx}, \tag{4.46}$$

and

$$\sigma_{yz} = -\sigma_{zy} = \frac{\hbar\omega_{\|} e^2}{2A_o \tilde{m}} \sum_{mk_x} (f_{m,1,k_x} - f_{m,0,k_x})$$

$$\times \left[\frac{\hbar\varpi + \hbar\omega - i\Gamma}{F_+} + \frac{\hbar\varpi - \hbar\omega + i\Gamma}{F_-} \right]. \tag{4.47}$$

where, $\Delta_{m_\pm} = \hbar\varpi - \hbar\omega_{\|}^2 \Omega^2 / 2\varpi(\varpi^2 - \omega_{\|}^2) \pm \hbar\omega$.

4.4.3 Power spectrum

The conductivity components above are inserted into Eq. (4.1) and the sum over k_x states is converted to an integral. The resulting power spectrum is

$$P(\omega) = \frac{\hbar^2 e^2 E^2}{8\pi L_y \tilde{m}} \sum_m \int dk_x \Omega \frac{f_{m+1,0,k_x} - f_{m,0,k_x}}{\hbar\Omega - \Theta}(m+1)\left[\frac{\Gamma}{\Delta_+} + \frac{\Gamma}{\Delta_-}\right]$$

$$+\frac{f_{m,1,k_x} - f_{m,0,k_x}}{\hbar\varpi + \Delta}\left[\Omega'\left[\frac{\Gamma}{F_+} + \frac{\Gamma}{F_-}\right] + 2(\omega_{\models} - \omega_{||})\left[\frac{\Gamma}{F_+} - \frac{\Gamma}{F_-}\right]\right], \qquad (4.48)$$

where $\Omega' = \omega_{\models}^2 + \omega_{||}^2 + \varpi^2/\varpi$ and $\Theta = \hbar\omega_{||}^2\Omega^2/2\varpi(\varpi^2 - \omega_{||}^2)$.

4.5 Magnetic field in the (y-z) plane of a wire with finite thickness

4.5.1 Velocity matrix elements

The velocity matrix elements are found using the velocity operator

$$[v_x, v_y, v_z] = -\frac{1}{m}\left[\imath\hbar\frac{\partial}{\partial x} + eB_{\models}z - eB_{\perp}y, \imath\hbar\frac{\partial}{\partial y} + eB_{||}z, \imath\hbar\frac{\partial}{\partial z}\right] \qquad (4.49)$$

and the wave function of Eq.(2.57). The results are

$$\langle n, k_x|v_y|n'k_x'\rangle \quad = \frac{\imath\hbar}{\tilde{m}\tilde{l}}\left[-\sqrt{\frac{n'}{2}}\delta_{nn'-1} + \sqrt{\frac{n'+1}{2}}\delta_{nn'+1}\right]\delta_{mm'}\delta_{k_x,k_x'}, \quad (4.50)$$

$$\langle nk_x|v_z|n'k_x'\rangle \quad = \frac{\imath\hbar}{m^*\tilde{l}_z}\left[-\sqrt{\frac{m'}{2}}\delta_{mm'-1} + \sqrt{\frac{m'+1}{2}}\delta_{mm'+1}\right]\delta_{nn'}\delta_{k_x,k_x'}. (4.51)$$

4.5.2 Conductivity tensor

The matrix elements (4.50)-(4.51) are inserted into Eq. (4.3) along with the eigenvalue of Eq. (2.57) and Eq. (2.58). We consider only the $n = 0$ subband again because of the strong confinement in the z-direction. The conductivity tensor is

$$\sigma_{xx}^{(nd)}(\omega) = \frac{i\hbar^2 e^2}{2A_o\tilde{m}} \quad (4.52)$$
$$\sum_{mk_x}\left[\frac{\omega_{\models}^2}{\omega_z}\frac{(f_{1,n,k_x} - f_{0,n,k_x})}{\hbar\omega_z + \Delta_z}\left[\frac{\hbar\omega_z + \Delta_z + \hbar\omega - i\Gamma}{H_+} - \frac{\hbar\omega_z + \Delta_z - \hbar\omega + i\Gamma}{H_-}\right]\right]$$

$$+\left[\frac{\omega_\perp^2}{\varpi}\frac{(f_{0,n+1,k_x} - f_{0,n,k_x})}{\hbar\varpi + \Delta}(n+1)\left[\frac{\hbar\varpi + \Delta + \hbar\omega - i\Gamma}{F_+} - \frac{\hbar\varpi + \Delta - \hbar\omega + i\Gamma}{F_-}\right]\right]$$

where $\Delta = (m + 1/2)\hbar\omega_{||}^3\Omega^2/\varpi^2(\varpi^2 - \omega_{||}^2)$, $F_\pm = (\hbar\varpi + \Delta \pm \hbar\omega)^2 + \Gamma^2$, $H_\pm = (\hbar\omega_z + \Delta_z \pm \hbar\omega)^2 + \Gamma^2$. All other conductivity terms are found following the procedure of the previous sections.

4.5.3 Power spectrum

The conductivity components above are inserted into Eq. (4.1) and the sum over k_x states is converted to an integral. The power spectrum becomes

$$P(\omega) = \frac{\hbar^2 e^2 E^2}{8\pi L_y \tilde{m}} \sum_n (n+1) \int dk_x \frac{f_{0,n+1,k_x} - f_{0,n,0,k_x}}{\hbar\varpi + \Delta} \left[\frac{\Omega_- \Gamma}{F_+} + \frac{\Omega_+ \Gamma}{F_-} \right]$$

$$+ \frac{f_{1,n,k_x} - f_{0,n,k_x}}{\hbar\omega_z + \Delta_z} \left[\frac{\Omega'_- \Gamma}{H_+} + \frac{\Omega'_+ \Gamma}{F_-} \right] \tag{4.53}$$

where $\Omega_\pm = \omega_\perp^2 \pm 2\varpi\omega_\perp^2 + \varpi^2/\varpi^2$ and $\Omega'_\pm = \omega_\models^2 \pm 2\omega_z\omega_\models^2 + \omega_z^2/\omega_z^2$

4.6 Conclusion

The power spectrum of the quantum wire seems to behave the same regardless of whether an anharmonic confinement potential is present or not. This seems to not follow from an intuitive standpoint. However, there is some small shift of the power spectrum along the x-axis when higher order terms are present. In the paper by Lorke et al. [26] the shift is shown experimentally, albeit for edge states in the quantum Hall regime of a 2DEG. These edge states are effectively one-dimensional and their confinement is shown to be mostly harmonic with the presence of higher order terms. The problem lies in the fact that the confining potential seems to be very dependent on the magnetic field and so difficult to model in a general sense.

If we were to look carefully at Eq.(4.12) and all subsequent equations for the power-spectrum we notice that the Lorentzian broadening is the dominant term in the power spectrum result. In that term, Γ will determine the width and the height of the power-spectrum peak, and because $|\Delta_{n+1}, k_x - \hbar\omega| \ll \Gamma$, when Γ is a constant or dependent on k_x, then the graphs will always be very similar. Furthermore, when Γ is not a constant we know from the d.c. conductivities that the dominant term in the relaxation time will be the magnetic field. The result is that the power-spectrum calculation is not a sufficiently sensitive test of the effect the addition of an anharmonic term would have on the electronic properties of the wire. In order for these terms to have an appreciable effect on the power spectrum, they woud have to contribute more than 20% to the energy. This again will lead to an equation that would make the use of perturbation theory less reliable.

Chapter 5

Conclusion

In the first part of this work we solved the one-electron Schrödinger equation for various orientations of the magnetic field. The confinement potential of the wire is modeled using the harmonic potential with small corrections. The Schrödinger equation was solved using the separation of variables method, with the non-harmonic terms dealt with using perturbation theory.

The energy eigenvalues are used to find the density of states (DOS), which must be solved numerically, save for the simplest case, the harmonic potential. The DOS is found to change very little, with any change in the parameter λ and γ, which describe the relative strength of the non-harmonic terms. This results in very little change to the Fermi level with respect to these same parameters. Therefore, all further calculations can be simplified with the assumption that the Fermi level for

the harmonic case alone may be substituted into the calculations.

The conductivity tensors we found using the Kubo-Greenwood formulas, which makes use of the single-electron wave functions and eigenvalues. The d.c. conductivity was found for several different scattering mechanisms, both elastic scattering by impurities and inelastic scattering by phonons. The harmonic case can be simplified to show the dominant term in all the scattering mechanisms to be the expectation values of the velocity and position operators. Since both cases are dependent on the magnetic field and because of previous assumptions about the wave functions, the non-harmonic terms in the confinement potential will not affect the conductivities appreciably. In order for the conductivity to be affected by the corrections, the contribution of the parameters λ and γ, would have to be on the order of the magnetic field contribution. This would mean that we could no longer use perturbation theory to solve the Schrödinger equation.

The d.c. conductivity for the non-harmonic case must be found using entirely numerical methods. This contradicts the assumption that using small corrections to the confinement potential would leave the equations analytically tractable. As a result, the calculation of the conductivites is not simplified with respect to the completely numerical results of the self-consistent theory.

The power spectrum analysis of the quantum wire measures the wire's response to an a.c. current. In strong magnetic fields the non-diagonal term in the conduc-

tivity is sufficient to find the power spectrum. As a result, the power spectrum can be put into the same form regardless of whether the non harmonic terms are present in the confinement potential or not. Essentially, there is no great formal difference when comparing the results of the harmonic confinement potential to the non harmonic one.

The prime motivation of this thesis had been to determine if modeling the confinement potential of the quantum wire, using higher-order corrections to the harmonic potential, would give a closer approximation to the actual result than simply using the harmonic potential. Furthermore, it was assumed that this would simplify the theory compared to the almost purely numerical calculations used in the self-consistent theory. To the extent that the correction to the wave function was not evaluated, the simplification obtained is not sufficient as the small corrections do not change the results of the harmonic problem appreciably, nor are the equations sufficiently simplified when compared to the self-consistent theory. However, we know from experimental results [26, 27] that the confining potential is not harmonic, but exhibits anharmonic properties with a dependence on the magnetic field. Therefore, for the results found in the thesis to agree with these experimental results, the cubic and higher-order terms would have to be made considerably stronger. Meaning either that the correction due to the wave function must be evaluated before definite conclusions are reached or that we could no longer use

perturbation theory to solve the Schrödinger equation and so either way we must resort to a numerical solution again.

5.1 Further Study

The attempt to model the quantum wire comprised of studying the response of the wire to d.c. and a.c. currents using the single-electron approximation. While using the non harmonic terms does not simplify the self-consistent theory by making the results anymore analytically tractable, it may greatly simplify the numerical results and computing time. While using self-consistent calculations to determine the confinement potential, gives the closest approximation to the true form of the potential, solving the Schrödinger equation simultaneously with Poisson's equation is computationally very heavy. Therefore, it might prove to be useful to get an approximate form of the potential using a polynomial and then using this to solve for the eigenvalues and wave functions of the single-electron Schrödinger equation. Also, while not spoken about in this thesis, electron-electron interactions (which is a many body problem) could be dealt with in a Hartree manner. Using an approximate, confining potential might therefore greatly simplify the numerical calculations while giving a better representation of the quantum wire's response to applied external fields.

Bibliography

[1] C. Weisbuch, B. Vinter. *Quantum Semiconductor Structures, Fundamentals and Applications.* Academic Press, Boston, 1991

[2] M.J. Kelly. *Low Dimensional Semiconductors, Materials, Physics Technology, Devices.* Oxford University Press, New York, 1995

[3] J.H. Davies. *The Physics of Low Dimensional Semiconductors, An Introduction.* Cambridge University Press, New York, 1998

[4] L. Samuelson et al. , phys. stat. sol. **152**, 269 (1995).

[5] T. Suzuki and T. Ando , Journal of the Physical Society of Japan **62**, 2986 (1993).

[6] Qin Li and D.J. Thouless , Phys. Rev. Letters **65**, 767 (1990).

[7] T. Jungwirth and L. Smrcka, Journal of the Physics: Condensed Matter **5**, L217 (1993).

[8] B.H. Bransden and C.J Joachain. *Quantum Mechanics, Introduction to.* (Longman Scientific and Technical, New York, 1989)

[9] W. Greiner. *Quantum Mechanics, An Introduction.* (Springer-Verlag, New York, Third edition)

[10] E. Butkov. *Mathematical Physics.* (Addison-Wesley, Reading, 1968)

[11] N.W. Ashcroft, N.D. Mermin. *Solid State Physics.* (Saunders, Fort Worth, 1976)

[12] I.S. Gradshteyn, I.M. Ryzhik *Table of Integrals, Series, and Products.* editor A.Jeffrey,(Academic Press, New York, Fifth edition)

[13] K. Oto et al. , Proc. Int. Conf. Quantum Devices and Circuits, Alexandria, Egypt (1996).

[14] K. Oto et al. , Proc. 12th Int. Conf. Applied High Magnetic Fields in Semiconductor Phys., Würzburg, Germany (1996).

[15] J.H. Oh, Phys. Rev. B **48**, 15441 (1993).

[16] J. Hu and A.H. MacDonald, Phys. Rev. B **46**, 12 554 (1992).

[17] O. Madelung. *Solid State Theory, Introduction to.* (Springer-Verlag, New York, Third Edition)

[18] J.M.Ziman. *Principles of the Theory of Solids.* (Cambridge University Press,Cambridge, 1972)

[19] M. Charbonneau, K.M. Van Vliet, and P. Vasilopoulos, Journal of Mathematical Physics **23**(2),318 (1982).

[20] T. Ando, A.B. Fowler and F. Stern, Reviews of Modern Physics **54**,437 (1982).

[21] F.M. Peeters and P. Vasilopoulos, Phys. Rev. B **46**,4667 (1992).

[22] P.Vasilopoulos, Phys. Rev. B **32**,771 (1985).

[23] P.Vasilopoulos, Phys. Rev. B **33**, 8587 (1986).

[24] P.Vasilopoulos et al, Phys. Rev. B **35**, 1334 (1987).

[25] N. Mori et al, Phys. Rev. B **45**, 4536 (1992).

[26] A. Lorke et al, Phys. Rev. B **53**, 1054 (1996).

[27] Ch. Lienau et al, Phys. Rev. B **58**, 2045 (1998).

[28] W.H. Press et al. *Numerical Recipes (Fortran).* (Cambridge University Press, New York, 1989)

[29] D.M. Etter *Structured Fortran 77 for Scientists and Engineers-3rd ed.*(Benjamin/Cummings Publishing Company,Inc. Redwood City, 1990)

[30] A.L. Garcia *Numerical Methods for Pysics.* (Prentice Hall. Englewood Cliffs,1994)